Contract No.:

This manuscript has been authored by Battelle Savannah River Alliance (BSRA), LLC under Contract No. 89303321CEM000080 and/or a predecessor contract DE-AC09-08SR22470 with the U.S. Department of Energy (DOE) Office of Environmental Management (EM).

Chemical Understanding of Actinide Separations

Anna G. Servis*, Michael J. Servis†, Kevin P. McCann$^{\Phi}$, Mark P. Jensen$^{\delta}$, Jenifer C. Shafer$^{\delta}$

*Chemical & Fuel Cycle Technologies Division, Argonne National Laboratory, Argonne, IL, 60439, USA
†Chemical Sciences & Engineering Division, Argonne National Laboratory, Argonne, IL 60439, USA
$^{\Phi}$Weapons Production Technology, Savannah River National Laboratory, Aiken, SC, USA
$^{\delta}$Department of Chemistry, Colorado School of Mines, Golden, CO, USA

Keywords: Actinide, Separation, Solvent Extraction, Ion Exchange, Pyroprocessing, Computational Modeling

Abstract

This article provides a broad overview of the separation processes used to isolate actinides and the experimentally and computationally determined chemical characteristics that define those separations. The redox chemistry of the actinides plays a pivotal role in both aqueous and pyrochemical processing separations. The near-overlapping energies of the 6*d* and 5*f* orbitals in the light actinides allows for facile adjustment of actinide oxidation states, which is used in many established separation methods. In contrast, the stable, generally 3+oxidation states of the mid- and heavy actinides can make them difficult to separate from the similarly lanthanides(III). In aqueous separations, the tendency of the actinides to form anionic and neutral aqueous complexes with a variety of complexants (especially soft donors) is used to achieve high separation factors between chemically similar elements in both solid-liquid separations and liquid-liquid extraction. This selectivity can be further tuned through the use of specialized organic or solid phase ligands. Pyroprocessing separations utilize the unique redox behavior of the actinides to adjust their distribution between a molten salt electrolyte and either a solid electrode or molten metal phase. Atomic-level insights into the mechanisms underlying actinide separation processes, with the ultimate goal of predicting separation behavior, can be provided by electronic structure and statistical mechanical-based calculation methods.

1) INTRODUCTION

Chemical separations have been at the heart of understanding actinide chemistry since the elements were discovered. The original isolation and identification of actinides required precise chemical separations to isolate the small quantities of actinide materials generated. Since that time, many basic inferences about *f*-element chemistry have been derived from actinide behavior in separation applications.

The applications of actinide-containing materials are numerous, but generally center on their nuclear properties. Unlike the stable lanthanide series of 4*f*-elements, whose unique electronic structures find use in superconductors, magnets, alloys, and lighting, the radioactivity of the actinides limits their utility in many conventional applications. Instead, the nuclear properties of the actinides are exploited for generation of nuclear energy, medical diagnostics and therapeutics, oil well logging and radiothermal generators. In addition to nuclide production, the radiological hazard posed by many actinides necessitates their separation from waste streams or the environment. As a result, chemical separations remain a focus of research in actinide science.

In this document, we cover the essential characteristics of actinide chemistry as it pertains to their separation from a wide range of chemical media and for a variety of applications. The most commonly used methods for actinide separations rely on solid-liquid and liquid-liquid equilibria, either for aqueous solutions (adsorption, solid phase extraction and liquid-liquid extraction) or molten salts (pyroprocessing by electrorefining and molten salt extraction). A brief introductory overview of actinide chemistry is provided,

followed by a critical evaluation of the advantages and disadvantages of each separation method. The separation methods, their history, and selected applications are then described in detail. Finally, the role of computational modeling in the development and understanding of actinide separations is described, followed by a review of important computational methods and their applications.

1.1) Essential Actinide Chemical Characteristics

In 1945 Glenn T. Seaborg proposed the actinide concept along with his announcement of the discovery of two new elements, americium and curium.[1] Until then, the elements Th, Pa, and U had been placed under Hf, Ta, and W in the periodic table due to Th, Pa, and U having similar chemical properties. However, the newer elements Np, Pu, Am, and Cm did not follow the periodic trend. Seaborg surmised that a second transition series would follow Fr and Ra in the same way the 4*f* lanthanide series followed Cs and Ba. The new series would be the 5*f* actinide series, beginning with actinium. Applying this concept, Seaborg and his team was able to separate and identify Am and Cm by assuming similar chemical behavior as their lanthanide homologs Eu and Gd.[2]

The chemistry of the light actinides (Ac to Pu) is complex due to the close energies of the 6*d* and 5*f* orbitals compared to their counterpart lanthanide's 5*d* and 4*f*. In fact, for the lightest actinides, the 6*d* orbitals are lower in energy than the 5*f* orbitals, which causes thorium's ground state configuration to be $6d^2 7s^2$. Currently there is no evidence indicating thorium metal or ions contain 5*f* electrons.[3] Moving across the series, the energy of the 5*f* orbitals decreases, eventually becoming lower than the 6*d* orbitals. The change causes plutonium's ground state to be $5f^6 7s^2$. The energy of the 5*f* orbitals continue to drop across the series, which results in heavier actinides generally displaying more lanthanide-like behavior.[4,5] For this reason, the light actinides have more *d*-block behavior and can reach different oxidation states whereas heavier actinides are generally 3+ oxidation state, Figure 1, (*see* eibc0001).

Ac	Th	Pa	U	Np	Pu	Am	Cm	Bk	Cf	Es	Fm	Md	No	Lr
					2+	2+			2+	2+	2+	2+	**2+**	
3+	3+	3+	3+	3+	3+	**3+**	**3+**	**3+**	**3+**	**3+**	**3+**	**3+**		**3+**
	4+	4+	**4+**	4+	**4+**	4+	4+	4+	4+					
		5+	5+	**5+**	5+	5+	5+							
			6+	6+	**6+**	6+								
					7+	7+								

Figure 1: Accessible oxidation states of the actinides (common oxidation states in **bold**).

Separation schemes such as PUREX (Plutonium Uranium Reduction Extraction) capitalize on the varied oxidation states, high charge densities and high coordination numbers of the early actinides. In the PUREX process uranium(VI) as a linear dioxocation, UO_2^{2+}, and plutonium(IV) are extracted from nominally 4 M HNO_3 into a kerosene diluent containing tributyl phosphate. The tributyl phosphate coordinates with the UO_2^{2+} and Pu^{4+} through a solvating mechanism and partitions into the organic phase.[6–8] The lanthanides and actinides in 3+ oxidation state remain in the aqueous phase (*see* eibc2528, eibd0653).

1.2) Motivating Factors

The choice of actinide separation process is heavily impacted by considerations of scale, initial matrix, final purity, waste generation, and safety. Many of the earliest actinide separations relied on precipitation to produce purified chemical compounds. The first actinide identified as a distinct element was uranium, which was isolated as the oxide from pitchblende ore by precipitation in 1789 (*see* eibc2525).[9] Also, notably, the isolation of plutonium following its discovery in 1940 was first achieved in 1942 by co-precipitation with rare earth fluorides.[10] Because they require only some means of filtration to separate phases, precipitation processes are straightforward to implement and can produce solid compounds of high purity from complex mixtures through the formation of uniform crystals. However, due to small separation factors between elements, many actinide separation processes require multiple fractional precipitations with carrier elements, resulting in a substantial amount of time and effort required for the separation as well as the

production of large volumes of radioactive waste. Separation factors in solid-liquid separations are calculated by dividing the concentration of an element in the solid phase by that in the liquid phase for two different elements, then dividing the larger value by the smaller one.[11] A separation factor greater than one indicates that the elements can be separated. Precipitation processes are generally preferred only when the desired purity can be reached in a single step.

Liquid-liquid extraction is a highly selective separation method and many extractive separations have higher separation factors than solid-liquid partitioning methods.[12] Liquid-liquid extraction separation factors are calculated like solid-liquid separation factors except that the organic phase concentration is substituted for the solid phase concentration. The ease of liquid handling and phase separation in industrial operations makes continuous multistage liquid-liquid extraction processes straightforward to design and implement for large scale separations. However, they can be onerous to perform at a laboratory scale due to the time and equipment required to manually contact and separate coexisting liquid phases, particularly in separations requiring multiple contacts. Furthermore, the use of organic solvents, like highly volatile and explosive diethyl ether used historically to recover uranium, can introduce serious chemical and physical hazards. The volume of waste resulting from liquid-liquid extraction is often small compared with other methods due to recycling of the solvent, making it attractive for radioactive waste management.[13,14]

Solid-liquid partitioning processes based on adsorption and solid phase extraction are highly effective for laboratory-scale separations. Multistage separations are easily implemented by packing a column with the solid phase material and running a sample through the column, while, much like precipitation methods, separation of the liquid and solid phases is immediate and complete. Solid-liquid partitioning processes are usually transient; a mixture is first introduced to the solid bed or column in a discrete volume of liquid and the separated components are then eluted at different times using solutions of varying composition. Because the solid phase must be periodically regenerated, adsorption is rarely used in industrial-scale separations except to separate trace elements from large volumes of dilute solutions such that regeneration is needed only at long intervals.

Pyroprocessing methods for purifying actinides have been used to produce metallic uranium and plutonium of very high purity from irradiated nuclear fuel.[15–17] Electrorefining and molten salt extraction use molten salt electrolytes as solvents in processes that are analogous to conventional metallurgical electrowinning and liquid-liquid extraction, respectively. Unlike the organic solvents used in liquid-liquid extraction, these inorganic materials are not susceptible to radiolytic degradation. This means that irradiated nuclear fuel can be processed almost immediately after removal from a reactor without requiring a cooling-off period to allow the shortest-lived radionuclides to decay. Furthermore, the electrolyte solvents can be recycled indefinitely, resulting in a minimal volume of radioactive waste. The extreme conditions under which pyroprocessing must take place require the construction of unique remote operation, corrosion-resistant, and inert-atmosphere equipment, limiting its use to the recovery of valuable elements from highly radioactive materials.

2.) ADSORPTION AND SOLID PHASE EXTRACTION

Among the simplest methods of actinide separations are those based on the differential affinity of a solid phase for actinides and impurities in solution. Chemical separations based on solid-liquid equilibria have a history extending thousands of years due to the ease of their implementation and the availability of natural adsorbents including clays, soils and char. Ancient Egyptians and Greeks used activated carbon to treat medical disorders around 1550 B.C.E. and 460 B.C.E, respectively, while Phoenicians used the same material to remove

impurities from drinking water circa 460 B.C.E.[18] In the era following the Scientific Revolution to the present, the use of solid-liquid partitioning methods has been extended to include applications in fields as diverse as agriculture,[19] biology,[20] environmental remediation,[21] and radiochemistry using both naturally-occurring and synthetic organic and inorganic solid materials.

When a solution containing a mixture of elements is contacted with a high-surface area solid, ions diffuse to the surface of the solid and may be retained by either adsorption directly to the solid surface or extraction by a physisorbed liquid phase. Depending on the mechanism involved, elements partitioning by adsorption are held in the solid phase by relatively strong chemical bonds or weaker physical interactions between the dissolved metals and the solid. Ion exchange is the most important adsorption mechanism in actinide separations and is defined as the process by which ions in solution are reversibly bound to a solid through the displacement of sacrificial ions at the solid surface (Figure 2(a)). In a process that is here termed solid phase extraction, ions are selectively transferred to a liquid phase that is physically immobilized in the pores of the inert solid (Figure 2(b)). This separation method works based on the relative solubility of the ions in the two liquid phases. As used in the literature, solid phase extraction can also sometimes refer to any mechanism for uptake of a dissolved substance by a solid phase, including ion exchange.[22]

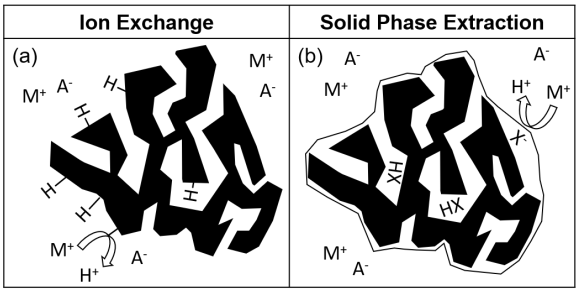

Figure 2: (a) Ion exchange occurs when a solution phase metal ion displaces an ion electrostatically bound to the surface of a solid. (b) Solid phase extraction is when a liquid phase physisorbed to a solid substrate dissolves an aqueous metal ion.

Separations effected by the partitioning of ions between a solid and liquid phase may be performed either in alternating adsorption and desorption (solid regeneration) cycles, or by the continuous flow of a liquid regenerant through a stationary bed of the solid substrate after adsorption, in a process known as chromatography. These two modes of operation are shown schematically in Figure 3 and are primarily used for bench scale actinide separations, although industrial processes have also been designed using these methods. The separation and recovery of elements in cyclic adsorption processes occurs by sequentially removing and replacing the liquid phase after each contact with chemically different solutions to alter the distribution of ions between the two phases. In chromatography, ions in solution flow through the length of a packed column at different rates due to differences in the affinity of the solid and liquid phases for each type of ion. Chromatographic separations can be approximated as a series of batch equilibrium stages, and a single column may have hundreds of theoretical plates allowing for complete separation of complex mixtures of chemically similar elements in one step.

Such chemical separations based on partitioning between a solid and liquid phase are defined by the energetics of the chemical equilibria between bulk solution and solid-bound species. The aqueous phase competes with the solid phase for ions, and the relative energetic favorability of the aqueous versus solid phase species determines the extent to which an element will be retained in each phase. In general, small, high charge ions will be strongly retained in the aqueous phase due to the strength of the electrostatic or hydrogen bonding interactions between the ions and water, aqueous counterions, or other complexants. Large ions also have large enough coordination spheres to be able to accommodate the number of extractant molecules and charge-neutralizing anions required for transfer from the aqueous to organic phases. Finally, the energy penalty associated with creating a cavity in water to accommodate small ions is less than that for large ions, leading to larger ions being more poorly retained in the aqueous phase. Equations 1 and 2 show the competing aqueous complexation and

ion exchange equilibrium reactions for a sulfonic acid functionalized cation exchange resin, R-SOOH, and an *n*-charged metal, M, in solution with a complexing counterion, X.

$M^{n+}_{(aq)} + nX^{-}_{(aq)} \rightleftharpoons MX_{n(aq)}$	(1)
$M^{n+}_{(aq)} + n(R\text{-}SOOH)_{(s)} \rightleftharpoons nH^{+}_{(aq)} + (R\text{-}SOO)_nM_{(s)}$	(2)

The application of solid-liquid partitioning to actinide separations is almost exclusively concerned with bulk aqueous electrolyte solutions in contact with particles of a synthetic organic polymer or inorganic solid phase.[23–26] These particles are tens to hundreds of micrometers in diameter, depending on application. Synthetic organic polymer substrates are commonly copolymers of styrene and divinylbenzene, which produce resins that are chemically resistant to molar concentrations of acids and bases. These materials have a high surface area and porosity, favorable swelling characteristics in aqueous solution, and can be surface functionalized or loaded with extractant solutions. Synthetic inorganic substrates like silica and zeolites tend to have poor stability in strong acid and base. However, they have been considered for industrial scale actinide separations due to their stability in high radiation fields and at high temperatures. When used as ion exchangers, the surface is often an activated form of the bulk material.

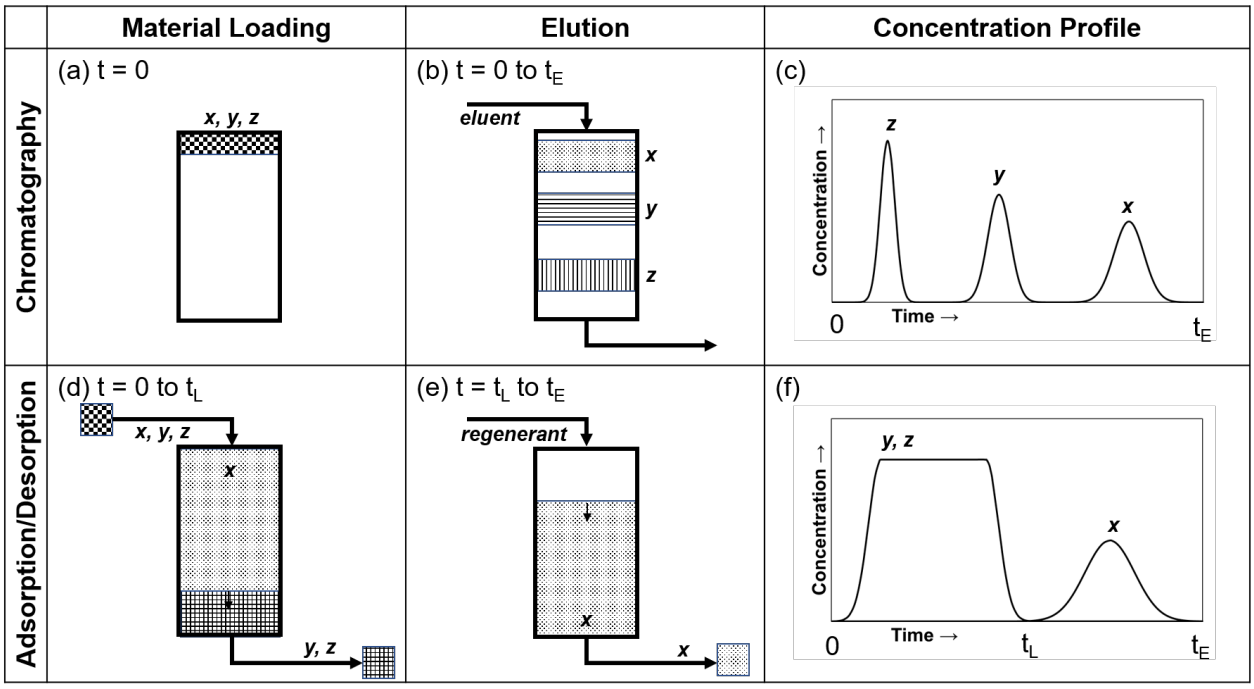

Figure 3: In chromatography, (a) a sample is loaded at the inlet of a packed column and (b) its components are separated on the column by elution with a mobile phase (c) such that pure fractions of each component are detectable at different times at the column exit. For cyclic adsorption/desorption, (d) the column is loaded with one or more elements until it is saturated and (e) the loaded elements are desorbed by a regenerant (f) to produce purified solutions.

2.1) Ion Exchange

In ion exchange applications, the surface of the solid phase includes covalently bound anionic or cationic functional groups that can exchange their electrostatically bound charge-neutralizing counterions. When the exchanged ion is positively charged these are termed cation

exchangers, and when the exchanged ion is negatively charged, anion exchangers. The most common functional groups on polymer resins are sulfonic acids (strong acid) and quaternary amines (strong base), although other acids and bases may also be used. Functional groups on inorganic materials include surface hydroxyl groups on silica or hydrous zirconium oxide. The same material may be an anion or cation exchanger depending on the pH of the surrounding solution, as observed for hydroxyl-bearing metal oxides that are cation exchangers at high pH and anion exchangers at low pH.

In dilute electrolyte solutions, the uptake of actinides by strong cation exchange resins is generally large due to the high, +3 or greater, effective ionic charges of their dominant solution phase species. The strength of the electrostatic interaction between the stationary, highly basic solid phase anions and hydrated solution phase cations controls uptake under these conditions, and any high charge cationic impurities will also be adsorbed.[27] However, this means that separations between ions of similar charge and geometry, such as lanthanide(III) and actinide(III), are difficult to perform under these conditions. As a result, ion exchange separations of chemically similar species are designed around either changing the solid phase functional group to improve selectivity or changing the aqueous phase environment to selectively disrupt or otherwise alter the nature of the interactions between the ions and the solid phase. Examples of this include developing specialized solid adsorbents with affinities for specific ions and adjusting the affinity of the ion for the solution phase by adding selective aqueous complexants.

This latter approach has been used at an industrial scale in the final purification and concentration of plutonium recovered from irradiated uranium by the PUREX process.[28] While the specifics of this anion exchange process have varied depending on facility, the general concepts underlying the separation, which occurs on a column of strong base resin at elevated temperature (60° C), are consistent. Plutonium exits the solvent extraction process in a dilute (<1 M) nitric acid stream with less than 1 g plutonium per liter and small amounts of uranium, fission products and corrosion impurities. The concentration of nitric acid in the stream is adjusted to between 6 and 7 mol/L HNO_3, where plutonium forms the strongly adsorbed $Pu(NO_3)_6^{2-}$ anion. The fission product and corrosion impurities are primarily 1st and 2nd row transition metals and these elements, as well as uranium, do not form strong anionic nitrate complexes. As a result, these impurities are poorly retained by the column and can be almost completely removed with a 7 M HNO_3 wash. This leaves only the plutonium adsorbed to the column, which is then eluted with dilute nitric acid for a final plutonium concentration as great as 63 g/L.

Aqueous-soluble organic molecules have also been used as complexants to increase ion exchange chromatography separation factors between chemically similar ions. This strategy has been used to separate americium(III) and curium(III) from each other in analytical applications. These separations are based on the slightly greater stability of aqueous phase complexes of smaller, heavier *f*-elements in 3+ oxidation state, which then move more quickly through a cation exchange column due to the increased competition of the mobile aqueous phase for those elements. The separation of Am(III) and Cm(III) from each other on a cation exchange column can be performed by elution using either lactic acid or tartaric acid solutions adjusted to approximately pH 4 with ammonium hydroxide.[29] The lactic acid separation takes less than 2 hours to complete, while the tartaric acid separation requires approximately 16 hours. Another commonly used aqueous complexant is ammonium α-hydroxy-isobutyrate, which is also effective at separating Am(III) and Cm(III) by cation exchange.[30]

Selective adsorption by functionalization of the solid phase has been explored for use in recovering uranium at parts per billion levels from seawater.[31] In work performed in the 1960s and 70s, hydrous titanium oxide was identified as the adsorbent with the highest capacity and selectivity for uranium relative the interfering ions found at high levels in seawater such as sodium, magnesium, and calcium. However, this inorganic adsorbent, which uptakes the uranyl carbonate anion in seawater according to the

equilibrium relationship provided in Equation 3, also adsorbs and concentrates substantial amounts of iron, vanadium, manganese and chromium even though these elements are found at very low concentrations initially.[32] A more recently developed strategy for optimizing uranium recovery is to improve the uranium selectivity of adsorbents by functionalizing the surface of porous inorganic substrates such as mesoporous carbon or silica with functional groups from organic ligands demonstrated to selectively bind uranium in solution. The most successful of these include carboxylic acid, phosphoric acid, and amidoxime functionalities.[33–35] Research in this area is ongoing to overcome the limited uranium capacities of these solid adsorbents, as well as the practical problem of how to contact a loose particulate solid material with millions of gallons of seawater.

$$UO_2(CO_3)_3^{-4} + Ti_x(OH)_{y(s)} \rightleftharpoons 2HCO_3^{-1}{}_{(aq)} + Ti_x(OH)_{y-2}UO^{2+}(CO_3)_3^{-2}{}_{(s)} \quad (3)$$

2.2) Solid Phase Extraction

Solid phase extraction (SPE) materials consist of a porous solid substrate loaded with the greatest amount of liquid extractant that can be supported while not forming a separate liquid phase.[36] This results in an extractant coating on the solid that is very thin relative to the volume of the solid, but large compared with the size of the extractant molecules. The most used SPE materials consist of styrene-divinylbenzene copolymer beads loaded with an extractant such as di-2-ethylhexyl phosphoric acid. Almost any water immiscible extractant can be used, although it must be sufficiently hydrophobic to be effectively retained by the solid. Because the separation mode of these materials is theoretically identical to that of liquid-liquid extraction, separation trends determined for liquid-liquid extraction systems can usually be extrapolated to SPE and vice versa. However, the direct mapping of theory developed for liquid-liquid extraction to the design of solid phase extraction separations is imperfect, and determining the reasons for this discrepancy remains an area of ongoing research.[37] A comprehensive description of the paradigms needed to fully understand solid phase extraction will be described later in the section on liquid-liquid extraction.

Solid phase extraction chromatography has found substantial success in the analytical separation of actinides. The separation factors achievable by liquid-liquid extraction for chemically similar elements can be much greater than those observed for ion exchange, and the packed column setup allows for many extraction stages in series at a laboratory scale. These benefits have been leveraged to separate Am(III), Cm(III), and the lanthanides(III) in individual fractions by the cation exchange extractant di-2-ethylhexyl phosphoric acid (HDEHP) loaded on a diatomaceous earth substrate to quantify fission yields.[38] In that process, the mixture of 3+ oxidation state elements in 0.15 M HCl is loaded on the HDEHP chromatography column and the elements are eluted in sequence from light to heavy by gradient elution with a steadily increasing HCl concentration in less time than that required for separation by ion exchange.

The separation and concentration of actinides by solid phase extraction is particularly useful for actinide analyses of environmental samples. Actinides in water, soils, and vegetation are usually found at low levels with many potentially interfering organic and inorganic compounds and their selective isolation and concentration is required for accurate quantification. A standard analysis for drinking water samples involves quantifying the gross alpha radiation emitted by naturally occurring isotopes of uranium, thorium, and their radium decay products.[39] In one such analytical method, an organic polymer substrate loaded with the actinide-selective cation exchange extractant, P,P'-di(2-ethylhexyl)methane diphosphonic acid (DIPEX) uptakes uranium and thorium from large, 100 mL drinking water samples adjusted to pH 2 with HCl.[40] The alpha-emitting elements are concentrated on 0.5 g of the resin while other inorganic and organic materials flow through the solid bed. The gross alpha radioactivity is then

quantified directly by liquid scintillation counting of the resin.

3) LIQUID-LIQUID EXTRACTION

Actinide separations based on liquid-liquid extraction rely on differences in the solubilities of actinides and impurities in two immiscible liquid phases (*see* eibc2529). These phases generally consist of a dense aqueous phase in contact with a less dense organic phase (Figure 4). Separations are based on the balance between the affinities of the aqueous and organic phases for an element. For example, in 1842 Eugène-Melchior Péligot reported the high solubility of uranyl nitrate in diethyl ether, reflecting the solvent's high affinity for the compound.[41] This knowledge formed the basis for the first industrial-scale liquid-liquid extraction process to produce purified uranium from dissolved ores in 1942.[42] The selectivity of diethyl ether for uranium is so great that a single extraction stage was required to produce uranium with only trace impurities.[43] However, such high selectivities are not required for effective separations, and even minor differences in organic phase solubility can be used to produce products of high purity in continuous multistage countercurrent flow liquid-liquid extraction processes.

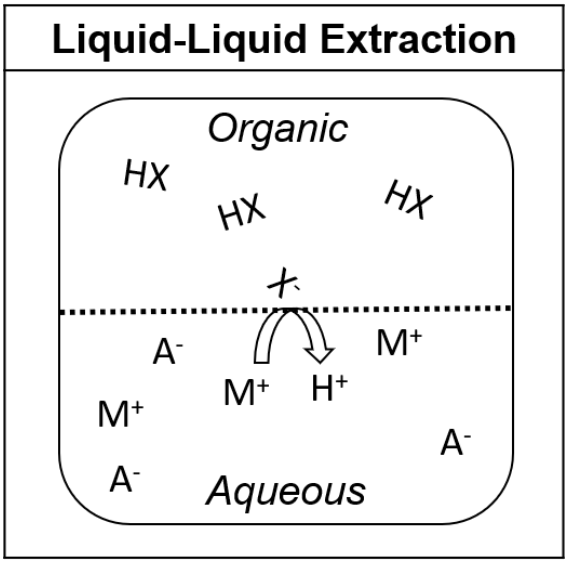

Figure 4: In liquid-liquid extraction, a metal ion is transferred from an aqueous to organic phase by interaction with an extracting molecule.

Organic and inorganic complexants are used to tune the affinity of the aqueous phase for different elements in liquid-liquid extraction, where the chemistry of the aqueous phase has a similar effect on separations as that observed in adsorption processes. Extractants, either as pure solutions or dissolved in an inert diluent, play an analogous role in the organic phase by interacting only with selected elements. There are two extraction mechanisms of substantial interest in actinide separations by liquid-liquid extraction: extraction by solvation and extraction by ion exchange. The latter is qualitatively identical to ion exchange in adsorbents, except that extractant molecules with ion exchange functionalities move freely in solution and are better able to evenly distribute around the coordination sphere of a metal ion than when bound to a solid phase. Separation trends for ion exchange extractants often closely follow those of ion exchange adsorbents. Extraction by solvation occurs when a neutral metal salt is extracted into the organic phase by a strong chemical interaction with a molecular extractant.

3.1) Extraction by Ion Exchange

Liquid-liquid extraction by cation exchange proceeds according to the equilibrium relationship in Equation 4, showing the extraction of an *n*-charged metal, M, by an acidic extractant, HX. Commonly used cation exchange extractants include β-diketones like thenoyltrifluoroacetone (TTA) and organophosphorus acids like HDEHP. The uptake of metal ions by β-diketones and similar extractants in the organic phase includes coordination of the metal by intramolecular carbonyl groups in addition to the exchange of the metal ion for protons. In contrast, extraction by organophosphorus acids is defined by the cation exchange process alone.

$$M^{n+}_{(aq)} + nHX_{(org)} \rightleftharpoons MX_{n(org)} + nH^{+}_{(aq)} \quad (4)$$

Equation 5 shows the extraction of an *n*-charged metal anion, M, by anion exchange with a tertiary alkyl ammonium salt, $R_3NH^+A^-$. Anion exchange extractants are usually tertiary or quaternary alkyl

amines converted to their ammonium salts by reaction with an acid. Examples include trioctylammonium nitrate, tridodecylammonium nitrate, and Aliquat 336 (methyltrioctylammonium chloride).

$$M^{n-}_{(aq)} + nR_3NH^+A^-_{(org)} \rightleftharpoons (R_3NH^+)_nM^{n-}_{(org)} + nA^-_{(aq)} \quad (5)$$

The organophosphorus cation exchange extractant HDEHP plays an essential role in the actinide-lanthanide(III) separations by phosphorus reagent extraction from aqueous complexes (TALSPEAK) process for actinide(III) and lanthanide(III) group separations.[44] Proposed schemes for minimizing radioactive waste and recycling nuclear fuel by partitioning and transmutation require the isolation of the lanthanides, which are neutron poisons, from irradiated fuel. The distribution of similarly-sized lanthanides(III) and actinides(III) between an HDEHP-containing organic phase and a non-complexing aqueous phase is nearly identical, and no separation is possible between these groups of elements with HDEHP alone, as shown in Figure 5.[45] The TALSPEAK process was developed in the United States and has been proposed for use after separation of the lanthanides and actinides from nuclear fuel by the transuranic element extraction (TRUEX) process.(Philip Horwitz et al. 1985; Moyer et al. 2015) TALSPEAK uses diethylenetriamine pentaacetate (DTPA) in a lactic acid buffer to preferentially complex the actinides(III) in the aqueous phase, causing them to be more poorly extracted than the lanthanides(III). This process can provide complete separation of the lanthanides from the actinides in a multistage liquid-liquid extraction process. The enhanced stability of the DTPA-actinide complexes has been explained using hard-soft acid-base (HSAB) theory, in which soft (larger, more polarizable) electron donors are observed to complex soft electron acceptors more strongly and vice versa (*see* eibc0251). Thus, the soft DTPA amine groups would be expected to interact more favorably with the softer actinides than the harder lanthanides, producing the observed separation.

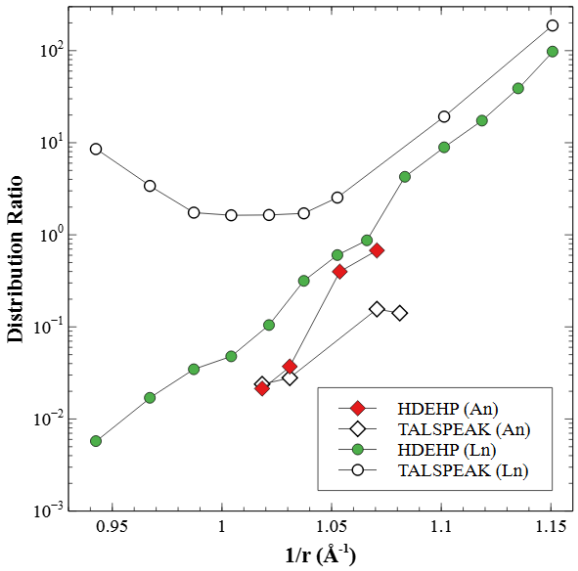

Figure 5: Separation factors between actinides(III) (An) and lanthanides(III) (Ln) with similar ionic radii, r, are small for an extraction system without an aqueous complexant (HDEHP/toluene from perchloric acid) and large for TALSPEAK (HDEHP/diisopropylbenzene from 1 M lactic acid/0.05 M DTPA)[45–47]

Tertiary amine anion exchange extractants have found widespread use in the mining industry for the recovery of uranium from ores. Most uranium mining relies on a three-step process to produce yellowcake uranium (primarily U_3O_8).[48,49] First, the finely ground ores are leached with sulfuric acid to create a pregnant leach solution (PLS) with elevated concentrations of uranium and other similarly soluble elements including copper, aluminum, iron, magnesium, and zinc. The PLS is then processed by liquid-liquid extraction using the Amex process to further purify and concentrate the uranium with a tertiary amine extractant such as Alamine 336.[50] Tertiary amine extractants have a high selectivity for

uranium, which forms anionic species with strongly-complexing sulfate, over the other constituents in ore. Only Zr(IV) and Mo(VI) are also extracted at appreciable levels. These impurities are removed in a H_2O_2 precipitation step yielding the final U_3O_8 product.

3.2) Extraction by Solvation

The extraction of a metal salt, MX, by a neutral solvating extractant, S, is shown in Equation 6, where *m* is the number of extractant molecules needed to dissolve the salt in the organic phase. These extractants work by coordination of the extracted metal cation with strongly basic carbonyl or phosphoryl oxygens. Prominent solvating extractants include ethyl ether, methyl isobutyl ketone, di-2-ethyhexyl isobutryamide, and tributyl phosphate.

$$MX_{(aq)} + mS_{(org)} \rightleftharpoons MX{\cdot}S_{m(org)} \quad (6)$$

The reduction-oxidation (REDOX) process for plutonium recovery uses the solvating extractant methyl isobutyl ketone (MIBK) to preferentially extract U(VI) and Pu(IV) from irradiated nuclear fuel dissolved in molar nitric acid.[51,52] After extraction, the plutonium is stripped from the organic phase by contacting with a dilute nitric acid solution also containing large amounts of aluminum nitrate, which salts out U(VI) and keeps it in the organic phase, and ferrous sulfamate, which reduces Pu(IV) to inextractable Pu(III). Finally, the U(VI) is stripped separately in dilute nitric acid. The REDOX process was used to produce plutonium at the Hanford Site in the United States between 1952 and 1967. In addition to being selective for uranium and plutonium, MIBK in its pure form has many favorable hydrodynamic characteristics that make it an attractive choice for use in continuous solvent extraction processes. The viscosity of MIBK is very low, comparable to that of water, and its density is low enough that it easily forms a separate, light organic phase after agitation with an aqueous phase. However, it also undergoes significant degradation on contact with nitric acid and has a low flash point (27 °C), which requires the construction of expensive, explosion-resistant facilities. These problems led to the REDOX process being abandoned in favor of the PUREX process, which remains in use today.

An alternative approach to separating the lanthanides(III) and actinides(III) for partitioning and transmutation is under development in Europe. The selective actinide extraction (SANEX) process aims to use fully incinerable solvating extractants containing only carbon, hydrogen, oxygen, and nitrogen (CHON) for this separation. Organophosphorus extractants are not fully incinerable and contribute to the volume of solid waste produced by hydrometallurgical processing of used nuclear fuel. The SANEX process uses aromatic polydentate, soft nitrogen-containing neutral ligands to selectively extract the actinides from a mixture of lanthanides(III) and actinides(III) in molar nitric acid produced by a preceding diamide extraction (DIAMEX) step. The early, alkylated bis-triazinyl pyridine (BTP) extractants developed for use in this process were prone to hydrolytic and radiolytic degradation in acid.(Kolarik et al. 1999; Modolo et al. 2012) Currently, two classes of closely related extractants are being developed with improved chemical stability and extraction kinetics: bis-triazinyl bipyridines (BTBPs) and bis-triazinyl phenanthrolines (BTPhens).(Love et al. 2019; Modolo et al. 2015) The addition of bridged bicyclic rings to BTP has also been found to reduce hydrolysis while maintaining high actinide(III)/lanthanide(III) separation factors.(Trumm et al. 2011)

3.3) Actinide(VI) Extraction

Group actinide(VI) extraction has received attention as a way to recover U, Np, Pu, and Am from used nuclear fuel in a single step. The

concept builds on the chemistry utilized in the PUREX process. As described previously, the PUREX process extracts uranium(VI) as the uranyl cation (UO_2^{2+}) from a molar nitric acid solution into an organic phase by the solvating ligand, TBP. A group actinide(VI) extraction seeks to oxidize U, Np, Pu, and Am to the 6+ oxidation state and extract all four actinides into an organic phase as their respective actinyl cations by a solvating ligand or by a co-crystallization method.[53–60] The primary challenge in the group actinide(VI) extraction concept is oxidizing americium(III) to the 6+ oxidation state. An Am(VI)/Am(III) redox potential of 1.68 V vs. SCE requires strong oxidizers to generate the americyl cation).[61] Early studies found Am could be oxidized to the 6+ oxidation state state using peroxydisulfate and silver nitrate catalyst in dilute acid solutions (<0.2 M HNO_3).[62] Oxidation of americium(III) to americium(VI) allowed americium to be separated from lanthanide(III) and actinides(III). As the linear dioxocation, AmO_2^{2+} forms a soluble species with fluoride or oxalate ions, similar to UO_2^{2+}, NpO_2^{2+}, and PuO_2^{2+}, whereas the lanthanides and actinides in the 3+ oxidation state form precipitates. In higher acid concentrations peroxydisulfate decomposed to peroxide which reduced americium(VI). The low acid concentrations required to quantitatively oxidize americium to the 6+ oxidation state are not conducive for liquid-liquid extraction processes like PUREX that require molar nitric acid for actinide(VI) separation to occur. However, the PUREX process was demonstrated on americium(VI) by oxidizing americium in 0.1 M HNO_3 with peroxydisulfate and silver nitrate.[53] The oxidized solution was then added to molar acid solution and contacted with TBP in n-dodecane. The studies showed the americyl ion is coordinated to two NO_3^- ions and two TBP ligands, analogous to uranyl, neptunyl, and plutonyl extractions.

Oxidation of Am^{3+} to AmO_2^{2+} in molar nitric acid has been demonstrated with the oxidizers $NaBiO_3$, Cu (III) periodate, and by electrochemical methods.[54,63,64] Extraction of AmO_2^{2+} oxidized by $NaBiO_3$ was demonstrated with TBP, diamyl amylphosphonate (DAAP), and monoamide solvating extractants in n-dodecane.[54,55,57] The DAAP extractant resulted in higher AmO_2^{2+} extraction compared to TBP due to the more basic phosphoryl group of DAAP. Extraction of UO_2^{2+}, NpO_2^{2+}, PuO_2^{2+}, and AmO_2^{2+} oxidized by $NaBiO_3$ showed uranyl has the highest distribution followed by NpO_2^{2+}, PuO_2^{2+}, and AmO_2^{2+} had the lowest distribution. Monoamide extractants were studied as a CHON ligand (incinerable). Additionally, branched chain monoamides are selective for actinyl ions over actinide(IV) ions such as Th^{4+}.[59,65] Extraction by the actinyl selective N,N-di(2-ethylhexyl)isobutyramide ligand showed same trend as DAAP where U > Np > Pu > Am.[57]

Oxidation by copper (III) periodate has the benefit of rapidly oxidizing Am compared to $NaBiO_3$ in molar acid and is soluble. Solvent extraction of AmO_2^{2+} oxidized by Cu^{3+} periodate was demonstrated with DAAP and monoamide ligands.[56,58,59] Although separation by 1 M DAAP was achieved, short contact times less than 10 seconds were required.[56,58] Distribution values decreased with extended contact times. The trend was observed both in $NaBiO_3$ and Cu^{3+} periodate oxidation schemes. Studies showed that upon contact AmO_2^{2+} began to reduce to less extractable species (AmO_2^+ and Am^{3+}).[58] The initial challenge to group actinide(VI) separations was to oxidize Am in molar nitric acid solutions required for liquid-liquid extraction process like PUREX. The ability to oxidize and extract americium(VI) in molar nitric acid has been demonstrated. The next great challenge is to maintain americium(VI) for extended times in mixed metal and high radioactive environments.

4) PLUTONIUM AND URANIUM PYROPROCESSING

Actinide pyroprocessing is a general term for processing nuclear material at elevated temperatures. High temperatures are necessary to keep salt, which acts as the solvent, in the liquid (molten) state in order to perform chemical separations. The three main processes associated with plutonium pyroprocessing are direct oxide reduction (DOR), molten salt extraction (MSE), and electrorefining (ER). DOR is not considered a separation technique in the classical sense because no purification occurs during the

process. Conversely, purification occurs in MSE and ER processes. Uranium pyroprocessing utilizes similar processes with the aim of processing used nuclear fuel to generate uranium fuel for commercial reactors.

4.1) Direct Oxide Reduction

Efforts to reduce plutonium into metal began with the Manhattan Project in the 1940's. Initially, uranium was used as a surrogate due to scarcity of plutonium material. The first plutonium material available for mg and gram production of plutonium metal were halide forms as PuF_3, PuF_4, and $PuCl_3$. The general reaction was to reduce the plutonium with calcium metal: $PuF_4 + 2\ Ca^0 \rightleftharpoons Pu^0 + 2\ CaF_2$. Plutonium's high density would theoretically cause the metal plutonium to coalesce at the base of the reaction vessel while slag would float to the top. A stationary reaction vessel and heated centrifuge method were initially tested. The centrifuge method used a metal centrifuge container that was heated to ~1000° C by induction heating and lithium was used as the reductant to produce 20 mg and later 520 mg of plutonium metal. The 20 mg was the first significant amount of plutonium metal made that could be seen with the naked eye. The stationary vessel was simpler and had fewer moving parts. Therefore, the stationary vessel was more ideal for plutonium reduction batches greater than 1 gram.[66]

Table 1: Reduction reactions for plutonium metal generation.[67,68]

Reactions	ΔH at 291 °K (kcal/mol Pu)	Slag Melt Point (°C)
$PuF_3 + 3/2\ Ca \rightleftharpoons Pu + 3/2CaF_2$	-54.8	1414
$PuF_4 + 2\ Ca \rightleftharpoons Pu + 2CaF_2$	-149.5	1414
$PuF_4 + 4\ Li \rightleftharpoons Pu + 4\ LiF$	-159.2	870
$PuF_4 + I_2 + 3\ Ca \rightleftharpoons Pu + CaI_2 + 2\ CaF_2$	-196.0	1320
$PuCl_3 + 3/2\ Ca \rightleftharpoons Pu + 3/2\ CaCl_2$	-56.0	772
$PuO_2 + 2\ Ca \rightleftharpoons Pu + 2\ CaO$	-52.4	2572

Reduction of PuF_4 by calcium was the most common method in the United States to convert plutonium halide into plutonium metal. For the reaction to produce high yields the slag products needed to remain molten long enough for the plutonium metal to coalesce. Reduction by calcium, with aid of an iodine booster, initiates around 600 °C and the heat produced by the reaction caused the reaction vessel to reach temperatures in excess of 2000 °C.[69] The amount of heat generated allowed the CaF_2 slag to remain molten long enough for molten plutonium metal to coalesce, and presence of CaI_2 decreases slag melting point (Table 1), further extending amount of time Pu metal can coalesce. Due to the low exothermic yield and high slag melting point, reduction of PuO_2 by calcium metal was not considered a viable option (Table 1). However, it was thought that using $CaCl_2$ as a flux to dissolve CaO product and lower slag melting point could generate plutonium metal, but early attempts proved unsuccessful.[70,71]

In 1969 Wade and Wolf were the first to demonstrate that large amounts of Pu metal could be produced in high yields through reduction of

PuO_2 by Ca with a $CaCl_2$ flux.[67,72] The $CaCl_2$ dissolves the CaO byproduct and has a solubility of approximately 18-mol%. High concentration of CaO in the solvent decreases viscosity and inhibits plutonium metal coalescence and phase disengagement. Application of PuO_2 reduction began in the 1970's in order to produce metal ^{238}Pu.[69] A drawback behind reduction of PuF_4 is the (α, n) reaction on F. The higher activity of ^{238}Pu exacerbated worker exposure to radiation whereas reduction of PuO_2 mitigated the dose issue. As a result, reduction of PuO_2 replaced PuF_4 reduction as the preferred method of generating metal plutonium and has remained relatively unchanged. In an effort to decrease amount of waste produced by DOR, the $CaCl_2$ slag containing up to 18-mol% CaO and 1-wt% Ca metal was converted to $CaCl_2$ by sparging phosgene, HCl, and/or Cl_2 in the molten slag.[73,74] Sparging Cl_2 through the molten slag to convert Ca and CaO to $CaCl_2$ was found to be the most efficient method, and salts were able to be re-used in DOR operations.[73] *In situ* regeneration of salt in the DOR process allowed for additional PuO_2 material and Ca metal to be added to reaction cell without the need to turn off, cool down, and recover the plutonium metal. As a result, less salt waste is generated per gram of plutonium metal generated by running multiple cycles of DOR before metal recovery and is aptly named MCDOR.[75] Whether using DOR or MCDOR, neither process purifies the plutonium material. Impurities in the oxide material go into the metal product. Purification of the plutonium metal requires additional processing.

4.2) Molten Salt Extraction

Depending on the type of plutonium isotope and isotopic purity, decay products such as ^{241}Am build up as a result of ^{241}Pu beta decay ($t_{1/2}$ = 14.3). The presence of ^{241}Am is a radioactive hazard for workers and affects the nuclear and mechanical properties of plutonium metal. Halide slagging was investigated as a method for purifying fission products from plutonium fuel.[76] The work demonstrated that lanthanides can be removed by mixing fissium alloy (a plutonium alloy containing non-radioactive fission products that simulate plutonium burn-up in a reactor) with a salt mixture of $MgCl_2$-NaCl-KCl at molten temperatures (700 °C). The $MgCl_2$ reacts with elements that form more stable chloride compounds, i.e. $LaCl_3$. The stable chloride species are recovered in the molten salt phase while elements remain in the metal phase. The distribution values of actinide elements between molten chloride salt containing $MgCl_2$ and metal plutonium alloys were measured at Argonne National Laboratory.[77] The study showed Np, Pu, and Cm favored the metal phase whereas Cf, Es, and Am favored the salt phase, indicating molten salt extraction (MSE) as a method to recover americium from plutonium metal.

The MSE process was further developed by Rocky Flats Plant (RFP) in 1967 to recover americium from aged plutonium.[78] Initially RFP operated a 2 stage crosscurrent extraction where plutonium metal was contacted with a equimolar KCl-NaCl salt mixture containing 5.7 mol% $MgCl_2$. The two stage crosscurrent could achieve 90% americium removal from kilogram masses of plutonium.[79,80] The method achieved 97% Pu recovery with some Pu metal being oxidized to $PuCl_3$ and some uncoalesced Pu metal remaining in the salt phase. However, the crosscurrent method contributed to large salt volumes that required further treatment to recover americium. RFP further optimized the system by using a 30 mol% $MgCl_2$, 35 mol% NaCl, and 35% mol% KCl salt mixture. Excess $MgCl_2$ would react with Pu to form $PuCl_3$ and decrease plutonium recovery. Therefore, the overall salt mass of the 30/35/35 mixture was lower than the initial 5.7/47/47 mol%.[79,80]

4.3) Electrorefining

The first electrochemical production of plutonium metal was demonstrated in 1944 through electrodeposition of $BaCl_2$-KCl-NaCl molten salt containing $PuCl_3$ at 660 °C.[81] The limited availability of $PuCl_3$ at the time restricted experiments to 50 mg demonstrations and eventually 1-g experiments. Due to the success of the bomb reduction methods of $PuCl_3$ (present day DOR) development of electrodeposition process ceased. The process was later applied to reprocessing Pu-10 atom% Fe reactor fuel.[82–84] The process utilized an equimolar mixture of NaCl and KCl containing 2 molar $PuCl_3$. The

reaction cell was a cylindrical high vitrified alumina crucible containing an inner alumina crucible cup cemented together. The plutonium feed of 100 – 300 grams was placed in the inner cup. The electrolyte salt mixture was contained within the crucible and the cell was heated to 700 °C in an inert helium gas atmosphere. A tantalum stirrer that served as anode was lowered into the central anode cup containing plutonium metal and either tantalum or tungsten ring located in the outer concentric circle served as the cathode. A 2 V potential was applied across the system. Plutonium in the anode cup was oxidized to Pu^{3+} and transported through the electrolyte to the cathode where it was reduced to Pu^0 where it dripped off the cathode and coalesced in the outer ring.[85] A representation of the process is shown in Figure 6. The 2.54 wt% Fe in feed material was found to be less than 0.02 wt% in the cathode ring. While most impurity concentrations decreased, the amount of tantalum increased when tantalum cathodes were used. As a result, tungsten cathodes were established as the superior cathode material. The amount of aluminum in the metal also increased due to reactions pertaining to alumina crucible. Nonetheless, the process demonstrated greater than 99.9% pure Pu metal could be produced through electrorefining (ER).

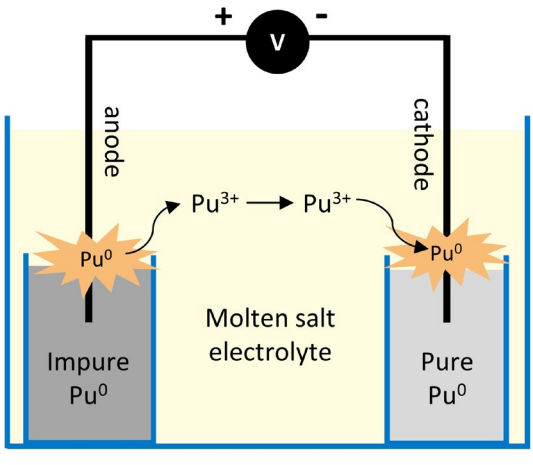

Figure 6: Electrorefining process showing impure plutonium metal oxidation at the anode, migration through the electrolyte salt, reduction back to metal at the cathode, and coalesces to form pure plutonium metal.

Electrorefining was further developed to process several kilogram amounts of impure plutonium at a time.[83,84,86–88] Instead of operating the cell under at constant 2 V, reaction cells were run at constant current. Initial trials showed currents above 6 amps resulted in tantalum contamination in the product due to dissolution of the tantalum stirrer/anode.[86] As a result, MgO stirrers were used and a separate anode rod with ceramic sheath was used to pass higher currents through the molten anode material.[82,86–88] Additionally, MgO crucibles were used due to their increased availability, and thus reduced the amount of Al contamination in the product.[8621]

During electrorefining as the amount of plutonium in the anode decreases, the concentration of impurities increases and increases the melting point of the anode slag. Terminating a run prior to the anode freezing with components in the melt is crucial for continued operations. To monitor the electrorefining progression, a back electromotive force (back-EMF or bEMF) was utilized to measure open circuit potential across the cell. As the concentration of plutonium in the anode decreases and an elevated bEMF value can be used to indicate when a run should be terminated.[82,83] The location and identity of impurities in the electrorefining cell is dictated by the Gibbs free energy of formation of metal chlorides (Table 2).[89] Metal chlorides with Gibbs free energies of formation per mole Cl less negative than $PuCl_3$ are not oxidized and remain in the anode. Metal chlorides more negative than $PuCl_3$ are oxidized and permeate into the molten salt. However, those metal chlorides tend to be more stable in the chloride salt and are not reduced at the cathode.[82,84,90,91] Using this process LANL was generating >99.9% pure Pu metal with approximately 83% yield.[87,90,92] The additional 10% remained in the anode and ~7% was $PuCl_3$ in the salt or uncoalesced Pu shot.[92]

Table 2: Gibbs free energy of formation per mole Cl^- at 1000K for various metal chlorides.

Metal Chloride	ΔG at 1000K (kcal/mol Cl^-)
$CaCl_2$	-76.7
NaCl	-76.2
$LaCl_3$	-66.1
$CeCl_3$	-64.5
$AmCl_3$	-60
$PuCl_3$	-58.6
$MgCl_2$	-58.0
$NpCl_3$	-54.1
$ThCl_4$	-53.4
UCl_4	-43.9
$GaCl_3$	-29.3
$TaCl_5$	-27.9
$FeCl_2$	-26.2
WCl_6	-8.8

Rocky Flats Plant integrated the electrorefining process into their operations around 1967.[93] The only major adaptation Rocky Flats made was to use $MgCl_2$ as an initiator material in place of $PuCl_3$. The use of $MgCl_2$ eliminated equipment and facilities needed to produce $PuCl_3$. The idea being, as in MSE, that $MgCl_2$ will react with Pu metal and form $PuCl_3$ in the molten salt mixture. Additionally, the $MgCl_2$ could be added to NaCl-KCl during a salt casting step, and the addition aided release of the casted block from the quartz mold.[93]

In the 1980's the plutonium metal production operations began trials to replace equimolar NaCl-KCl solvent with $CaCl_2$.[91,94] Initial motivation for a $CaCl_2$ ER system was to use common salts in throughout all Pu pyroprocesses and mitigate waste treatment strategies.[91,94] LANL demonstrated DOR, MSE, and ER processes using solely $CaCl_2$ salts. In 19 $CaCl_2$ runs, the average process yield was 74% compared to 73% for 323 runs with NaCl/KCl.[29] The early trials indicated $CaCl_2$ can be used to replace NaCl/KCl salt in the ER process. Studies out of Atomic Weapons Establishment (AWE) noted several benefits of $CaCl_2$ over NaCl/KCl salt.[95] The AWE studies showed an average yield of 90% with $CaCl_2$ compared to 74% with NaCl/KCl system. In the $CaCl_2$ system operating temperatures were run at 850 °C due to the 774 °C melting point of $CaCl_2$. Whereas equimolar NaCl/KCl has a melting point of 657 °C and operations typically run at 750 °C. Recall, as the plutonium is depleted in the anode the concentration of impurities increases. For anodes containing gallium, the anode will begin to solidify when the gallium concentration reaches 8.85 wt% Ga at 750 °C. Conversely, at 850 °C in the $CaCl_2$ system, the anode can reach 13.07 wt% Ga before solidifying. The higher operating temperatures allow more plutonium to be oxidized before onset of solidification and lead to higher percent yield.[95]

Chemical properties of Pu in molten salts were studied electrochemically.[96,97] The Pu^{3+}/Pu standard potential was found to be -2.54 V (vs. Cl^-/Cl_2 reference electrode) in NaCl/KCl system and -2.51 V in $CaCl_2$. The calculated activity coefficient for Pu^{3+} was larger in the $CaCl_2$ than it was in the NaCl/KCl system. The larger activity corresponds to a lower complexation by chloride ions. That is to say, the $CaCl_2$ complexes with Pu^{3+} species to a lesser degree than NaCl/KCl system. The differences in activity coefficients have an effect on the overall system, not just on Pu reduction potentials. A cyclic voltammogram of Pu^{3+} in NaCl/KCl on a tungsten electrode at 800 °C indicated reduction peaks at -2.8 V and -2.9 V. The -2.8 V was attributed to Pu reduction and -2.9 V was attributed to Na^+ reduction. This indicates the Pu and Na reduction potentials are close together and can lead to the production of Na metal and salt electrolyte degradation.[95,96] Conversely, the reduction potentials between $CaCl_2$ and Pu^{3+} were far enough apart to be considered separate phenomena. Changes in the reduction potential are also observed in distribution Am and Np impurities across the system. Recall from Table 2 the Gibbs free energy of $AmCl_3$ is higher than $PuCl_3$ and thus Am from impure feed will be oxidized into the salt phase. In practice, 93% Am removal was observed in $CaCl_2$ system while 70% removal

was observed in NaCl/KCl.[95] The hypothesis for this phenomenon is that the less complexing nature of $CaCl_2$ further separates the Am and Pu reduction potential causing Am species to not be reduced at the cathode and remain in the salt phase.

4.4) Uranium Pyroprocessing

Uranium pyroprocessing is an active field of research as a result of its application to process and purify oxide fuels from reactors.[98–100] Uranium pyroprocessing has been in practice since 1996 to process EBR-II (Experimental Breeder Reactor II). Flowsheets developed whereby used fuel is decladded and roasted to convert to oxide. The oxide is treated electrochemically to produce uranium metal. The uranium metal is further treated to remove residual salts. Lastly, the uranium is converted back into fuel pellets to be used in reactors. This section will focus on the electrochemical treatment.

Similar to plutonium electrorefining development, electrochemical synthesis of uranium metal began with uranium halide salts in molten salts. The first reported production of uranium metal in 1930 utilized KUF_5 and UCl_4 in NaCl-KCl melt with a 5 V potential between anode and cathode. Pure metal uranium deposited onto the cathode and was described as "tree-like".[98,101] During the Manhattan Project Kolodney worked on electrochemical production of plutonium metal.[81] Before plutonium was available, Kolodney tested UCl_3 in $BaCl_2$-KCl-NaCl molten mixture and deposited dendritic, silvery metal uranium on the cathode. He found that increased current density decreased the crystal size. Several other experiments demonstrated uranium electrodeposition in KCl-$BaCl_2$, LiCl-KCl, NaCl-KCl molten salts with UCl_3 and UF_4 material.[98,102] The reduction mechanism of UCl_3 was found to be a single three-electron transfer step.[103–105] Whereas UCl_4 reduction occurred via a two stage electron transfer. First a one electron reduction to U^{3+} followed by the three electron transfer for U^{3+}.[106,107] Studies by Chauvin determined the U^{3+}/U reduction potential to be -1.2 V in LiCl-KCl-UCl_3 mixture vs Ag/AgCl reference electrode.[108] The identity of alkali metal in the molten salt was found to effect the reduction potentials.[98] Studying LiCl, NaCl, NaCl-KCl, RbCl, and CsCl over varied temperatures showed the apparent standard electrode potential shifted in the positive direction with increasing temperature. Conversely, the potential shifted to more negative values as radius alkali cation increased as a result of the activity coefficients.

Electrolytic production of uranium metal from uranium oxides was demonstrated early in the Manhattan Project before bomb reduction by Mg became preferred process.[81,109] In the late 1950's the reduction of uranium oxide was reinvestigated.[110,111] Niedrach showed UO_2, UO_3, U_3O_8 could be reduced in BaF_2-MgF_2-UF_4 solvent at 1250 °C.[110] Similarly, Piper showed uranium in a UO_2-carbon pellet could be reduced in a BaF_2-LiF-UF_4 molten salt at graphite crucible at 1150 °C.[111] Reduction of uranium oxide was further demonstrated in the 2000's to expand electrometallurgical treatment operations at Idaho National Laboratory that treated EBR-II sodium-bonded uranium metal fuel.[112–114] The process reduces uranium oxide in molten LiCl-Li_2O molten salt (650 °C) to uranium metal. The reactions at the cathode and anode are shown in Figure 7.

Figure 7: Equations showing the uranium oxide reduction reactions that occur at the cathode and anode.

Cathode Reactions:

$$Li^+ + e^- \rightleftharpoons Li$$

$$UO_2 + 4\,Li \rightleftharpoons U + 2\,Li_2O$$

$$UO_2 + 4\,e^- \rightleftharpoons U + 2\,O^{2-}$$

Anode Reaction:

$$2\,O^{2-} \rightleftharpoons O_2 + 4\,e^-$$

In hot-cell demonstrations, MOX fuel is placed in stainless steel mesh baskets which act as the cathode and platinum wire is used as the anode and submerged in LiCl-1 wt% Li_2O molten salt (650 °C).[115] Elements such as Ba, Cs, Sr, and I

accumulate in the salt phase.[99,114,115] Actinide elements and some rare earths are reduced to metal in the process. As such, the electrolytic reduction process does not satisfactorily purify the uranium metal. An additional electrorefining process is needed to purify the metal, similar to plutonium pyroprocess purification. In uranium electrorefining, a LiCl-KCl eutectic containing UCl_3 initiator is melted at 500 °C. The reduced fuel in an anode basket and a cathode rod are submerged in the molten salt and a constant current is applied. The uranium is oxidized at the anode and is deposited onto the cathode. Across five rungs, the fraction of transuranic elements in the metal increased and the product became less dendritic. Studies using a liquid cadmium electrode showed a more cathodic potential increased the amount of lanthanides in the metal product.[116] To mitigate rare earth contamination, a liquid cadmium cathode with a large surface to volume ratio is necessary to decrease the current density at the interface and make the cathode potential less negative.

5) COMPUTATION MODELING AND ACTINIDE SEPARATIONS

With continuing advances in computational capabilities and method development, predictive modeling will play an increasing role in many domains of chemical science, including actinide separations. Modeling the chemistry of actinide separations requires a range of length and time scales, with computational methods depending on the target chemical behavior and desired chemical accuracy at that scale. For an actinide separations application where the relevant chemistry is often driven by dative interactions between a ligand molecule and an actinide ion, choice of an appropriate computational method depends on the plurality of accessible chemical states. Needing to account for more total relevant chemical states requires ensemble-based methods. Conversely, a narrow range of dominant molecular configurations reduces that need for ensemble methods and increases the importance of chemical accuracy for those predominant states. Therefore, the problem at hand determines the appropriate balance of chemical accuracy and statistical sampling. In the following sections we discuss the considerations demanded of high-accuracy electronic structure calculations and the computational options available for statistical mechanical methods.

5.1) Electronic Structure Calculations

Certain aspects of electronic structure calculations are more relevant for actinide-containing systems than more common calculations performed for systems composed only of light atoms, such as organic molecules. Due to the increased total number of electrons in actinides and the increased mass of the nucleus, frozen core potentials and relativistic effects are important. For *f*-elements, including actinides, there are a substantial number of core electrons which do not participate in bonding or otherwise contribute significantly to metal-ligand interactions. To reduce the already considerable computational expense of actinide atoms, core electrons---for actinides, as much as up to the 4*f* shell---are modeled with an effective core potential (ECP) rather than treated explicitly with the remaining valence electrons. For actinides, the Stuttgart ECP is commonly used.[117] Basis sets for valence electrons are developed specifically for use with corresponding effective core potentials. Heavy elements require treatment of spin-orbit coupling, which, due to computational expense, requires approximations such as the zeroth-order regular approximation (ZORA) or the exact two-component (X2C) relativistic Hamiltonian.[118] Spin-orbit coupling is particularly important for open-shell actinide systems.[119]

5.2) Statistical Mechanical Methods

Statistical mechanical-based methods generate ensembles of configurations through direct sampling of their relative energies (Monte Carlo methods) or by taking a time average of a system evolving with time (molecular dynamics). The latter assumes that the system is ergodic, meaning that all relevant states are sampled with sufficient statistical accuracy; the ergodic hypothesis states that the time average of a given property is equivalent to the ensemble average for a sufficiently long sampling time. Ensemble-based methods themselves span many length and time scales, with the fidelity of their physical and

chemical descriptions of intra- and intermolecular interactions varying accordingly. At the most detailed level, full electronic structure calculations (as described above) can be propagated in time using equations of motion to generate the ensemble of configurations. Such simulations are typically on the scale of 100s of atoms with trajectories up to 10s of picoseconds long. Alternatively, larger or longer simulations, applied to systems requiring more time to generate a statistical ensemble, empirically-derived potential energy descriptions are used instead. This approach has the benefit of computing interaction potentials between atoms using far more computationally inexpensive classical functions instead of electronic structure calculations. As expected, classical descriptions of the potential energy are less accurate and generally preclude certain behavior such as on-the-fly covalent bond breaking and formation, such as protonation and deprotonation reactions.

Given the challenges associated with describing the physical and chemical behavior of actinides, and, importantly, their lack of parameterization in common force fields---the set of potential energy functions and associated parameters which collectively represent all chemical and physical interactions---there are many different representations of actinides used in classical simulations with different degrees of transferability to common force fields. Generally, predominant considerations for studying actinides are the fundamental challenges associated with modeling high charge density ions: polarizability. The high charge density polarizes the electron density of nearby molecules, including any ligands, complicating the use of classical potentials with fixed atomic charges.

Various approaches exist for explicitly or implicitly modeling polarization. Non-polarizable force fields implicitly account for polarization in a mean field way, where the effects of polarization in condensed phases are averaged during the parameterization process. While a given property of an actinide ion may be fit in a given empirical force field, the challenge resides in developing a sufficiently robust potential energy description which captures enough of the underlying physical behavior to simultaneously model many of that ion's properties under a wide range of chemical conditions. Flexibility to capture more physical properties can be improved with explicit polarization models. One approach to modeling explicit polarization for actinide ions that has been implemented is the Thole model. This was used to study aqueous solution structure of actinide ions.[120–122] Force fields are typically developed under dilute, solution phase conditions. However, separations processes for non-analytical applications are not generally operated in the dilute limit and long-range interactions between highly charged actinide ions are necessary to accurately model their solution phase behavior. Spezia et al. propose that a simple extension of their force field parameters with typical mixing rules could be used to derive actinide-actinide interatomic potentials.[122]

These specialized actinide ion potentials demonstrate impressive chemical accuracy but are not without implementation challenges. In general, the variety in functional forms for potentials with explicit polarization limits the transferability of any such potentials developed for actinides. As a result, these models cannot always be simply incorporated into robust force fields that are extensible to arbitrary chemical systems, such as a solution with a ligand molecule of interest. To address this issue, Merz and coworkers developed so-called 12-6-4 potentials for metal ions,[123,124] including *f*-elements.[125] Using this approach, they demonstrated that several essential ion solvation properties (importantly, ion-water oxygen distance and hydration free energy) can be simultaneously achieved for a wide range of ions types, including the challenging-to-model actinides. This model is intended for use with common empirical water models (TIP3P, TIP4P-ew and SPC/E) and are transferable to common force field representations of ligand molecules by modifying the nonbonded ion-ligand $1/r^4$ term with the atomic polarizability of the various atom types on the ligand. However, while this approach is carefully calibrated for modeling aqueous solvation for common water models, the lack of explicit polarization in these ion models still fundamentally limits the types of physical

behavior which can be modeled. Ongoing work parameterizing actinide ion potentials[126,127] in the Atomic Multipole Optimized Energetics for Biomolecular Applications (AMOEBA) force field,[128] which models explicit polarization using multipole expansions, could provide transferable, polarizable actinide potentials for a force field with a sufficiently large parameter set to model a sufficiently wide range of chemical systems.

Molten salts are an important application of actinides for use in advanced reactors as well as pyroprocessing separations techniques.[129] As they are challenging materials to perform experimental work on, they are a particularly important application for computation.[130] Recent simulation studies have elucidating the solvation of actinide cations in molten salts. Detailed analysis of actinide coordination by chloride[129,131] and fluoride[130] anions have been reported. In addition to structural information, thermodynamic properties, including heat capacity and thermal conductivity, determine a mixture's ability to extract heat when used as a homogeneous nuclear fuel. With these properties, predictions can be made to identify molten salt mixtures which, e.g., maximize heat transfer while minimizing temperature.[131] Similarly, dynamic properties, including diffusion and viscosity, are simulation-accessible and provide insight into transport behavior relevant to pyroprocessing. Molten salts, including those containing actinides, have computational considerations which are unique from typical condensed phase applications. Owing to the small, ionic constituents of the molten salt, explicit polarization is generally incorporated into classical simulation potentials. Alternatively, ab initio molecular dynamics simulations have also been applied to actinide-containing molten salts,[129] naturally incorporating those effects with the first principles approach at the expense of simulation length and time scales.

5.3) Hybrid Methods

Ensemble and single-configuration electronic structure methods can be combined advantageously to leverage the benefits of both while mitigating their respective drawbacks. One such approach are hybrid quantum mechanical/molecular mechanical (QM/MM) methods which treat certain regions of a system with a full quantum mechanical electronic structure calculation and the rest with a classical empirical force field. Often, QM/MM optimization is performed for a region of interest (e.g., an actinide ion bound to a ligand) from a classical simulation, allowing detailed study of the ligand/metal complex without sacrificing explicit solvation. While implicit solvent methods such as COSMO[132] can account for the impact of solvent dielectric with a continuum model, and small solvent-containing clusters with continuum solvent models can often be sufficient, many details of solvation are not accounted for without explicit inclusion of large quantities of solvent molecules. For example, solvent packing around a metal-ligand complex or the stabilizing effect of short range, directional interactions such as hydrogen bonding are not easily recovered with continuum solvation methods.[133] QM/MM approaches avoid the loss or distortion of solvent effects that would occur in a gas phase ion/ligand cluster calculation. In this manner, the impact of the solvation environment can be incorporated (albeit at a classical level) while the quantum mechanical description of the actinide ion's local environment allows for computation of standard electronic structure-dependent properties, including adsorption or vibrational spectra.

Infante and Visscher studied solvation of uranyl fluoride complexes, finding that the energy difference between hexa- and hepta-coordinated uranyl depended on the number of explicit water solvent molecules up to 30 total water molecules.[134] This role of explicit solvation beyond the primary solvation shell highlights the potential for solvent-ligand and solvent-ion interactions to impact condensed phase energetics. In this case, decomposition of the uranyl complex and solvent into QM and MM regions provided a good compromise between computational efficiency and chemical accuracy, highlighting the benefit of a hybrid approach. Odoh et al. also studied the uranyl fluoride complex, considering its docking in a protein.[135] In addition to the importance of solvating waters as discussed above, modeling the protein cavity would not be possible without a MM treatment of

that protein. These studies highlight the types of systems which necessitate hybrid approaches.

5.4) Considerations of Chemical Environment

The chemical environment in which a given actinide separation process occurs dictates the computational approach. For example, for the same extracting ligand, whether a process is solid phase adsorption or liquid-liquid extraction impacts the utility of the different computational techniques discussed above. In solid phase adsorption, where the extracting ligand is covalently bound to a solid substrate such as a polymer backbone, arrangement of the ligand and any charge neutralizing anions around the actinide cation is relatively fixed. This is encountered in applications such as uranyl capture from seawater where uranyl-ligand binding can be modeled well despite only considering the first coordination shell of solvating water.[136] In this case, electronic structure calculations are effective because the available configuration of the ligand around the metal ion is constrained and therefore better represented by single lowest energy (geometry optimized) configuration.

By contrast, liquid phases are characterized by a multitude of accessible states. In liquid-liquid extraction, the actinide ion is distributed between two immiscible phases: one high dielectric and one low. The generally aqueous high dielectric phase plays an important role in actinide solvation free energy in that phase, but the correlation length of aqueous phases is generally short. That is, the high dielectric screening and small molecular lengths means that solvation effects can be achieved by accounting for relatively small regions of the solution phase. Conversely, low dielectric "oil" phases such as kerosene feature much larger solvent molecules with correspondingly larger correlation lengths. While solvent molecule sizes on the scale of n-dodecane quickly confound electronic structure methods, the low dielectric of such solvent phases and lack of strong direction interactions requiring explicit solvent models means that often simple continuum solvation corrections are sufficient.

However, some actinide separation processes occur in solutions which are characterized by strong, directional polar interactions and larger solution correlation lengths. While characterization of complex stoichiometries and associated geometries as well as, in particular, outer-sphere actinide solvation[137] or inter-complex[138] interactions are challenging to probe experimentally, these features are readily obtained from simulation. For these systems where numerous species are in equilibrium, statistical mechanical methods---rather than electronic structure calculations of a single composition and geometry---are an appropriate computational approach.

A quintessential example of such a system used in actinide separations is room temperature ionic liquids.[139,140] There, classical simulations are often applied to model the full range of solvation environments which contribute to actinide solvation in the ionic liquid. Due to molecule size and viscosity, classical nonpolarizable simulations are commonly used for these applications.[141] In the absence of computationally expensive explicit polarization, charge scaling of ionic species is commonly employed.[142] With this approach, Chaumont and Wipff and later Maerzke et al. investigated the relative stabilities of mixed water/ionic liquid solvation of actinyl ions, finding significant incorporation of water into the first solvation shell of the actinide despite the ionic solvent.[141,143] Overall, understanding solvation environment, including how important solvent molecules are to accurately model separations---and the length and time scales necessary to account for that impact---is a prerequisite for choosing the appropriate computational approach.

5.5) Predicting Ligand Binding and Separations Efficacy

The state-of-the-art accuracy of actinide electronic structure calculations depends strongly on system complexity. At present, relatively high accuracy has been achieved for properties such as reaction enthalpies for simple gas phase calculations of actinide-containing species, as illustrated in Figure 8. These results use computationally expensive post-Hartree-Fock

wavefunction-based methods, such as coupled cluster methods like CCSD(T) with correlation consistent basis sets.[144] Generally, these are performed as single point calculations on density functional theory (DFT)-optimized geometries. These calculations are remarkable for their chemical accuracy, but extension to more complex with more direct application to predicting separations is not trivial.

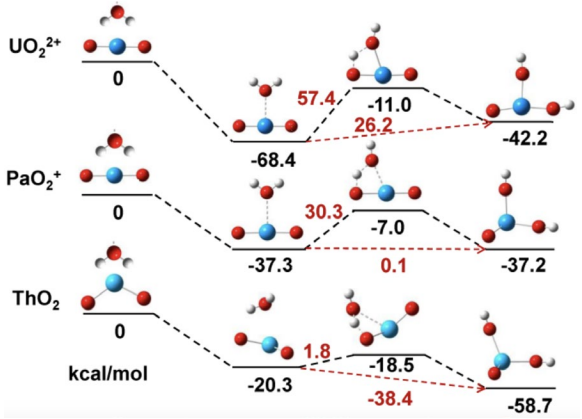

Figure 8: Reaction enthalpies for gas phase hydrolysis reactions are calculated for different actinyls to high accuracy using coupled cluster methods. Reprinted with permission from "Reliable Potential Energy Surfaces for the Reactions of H_2O with ThO_2, PaO_2^+, UO_2^{2+}, and UO_2^+," Vasiliu, M. and Peterson, K. and Gibson, J. and Dixon, D., J. Phys. Chem. A 2015, 119, 11422-11431. Copyright 2015 American Chemical Society.

Recent studies have endeavored to quantitatively predict fundamental properties of simple, gas phase actinide systems; we highlight some such studies here. The electronic structure and relative energies of a wide range of gas phase structures, including dioxide cations for various actinide oxidation states, were mapped out across the actinide series.[144] Similarly, study of the interactions of actinide oxide cations with simple ligand molecules have provided detailed information on energetics, geometry and vibrational frequencies of those clusters.[145,146] Comparison to experimental data shows that, while quantitative accuracy---a remarkable feat itself---is typically still a challenge, trends across the actinide series in accessible properties, such as vibrational frequencies and bond dissociation enthalpies,[147] can often be obtained through calculation.[118]

For more complex systems, quantitative accuracy remains a challenge. This includes calculations containing the extracting ligands, which aim to predict solvation free energies and therefore actinide distribution between phases. Typically, this is calculated by comparing electronic structure-derived free energies for representative actinide species in each phase, with the predicted distribution between phases corresponding to the Boltzmann factor for that energetic difference. For example, free energy differences were computed between complexation of the heavy actinides Am(III) and Cm(III) with a diglycolamide organic-soluble ligand and representative aqueous phase solvation of the actinide with coordinating water.[148] In this manner, the experimentally observable improvement in actinide extraction by diglycolamides with shorter alkyl tails was predicted, with the calculations demonstrating how this difference can be attributed to the steric impact of those tails when forming the actinide/nitrate/ligand complexes.

Absolute solvation free energies are often challenging to predict with computation. As a result, many calculations rely on careful error cancellation to minimize the error between two structures, such as those used to predict distribution between phases, so that the difference in those solvation free energies might be more accurate than the actual solvation free energies themselves. For example, owing to the similarity in error sources between solvation free energy calculations of Am- and Eu-containing metal-ligand clusters, Bryantsev and Hay reproduced trends in selectivity for Am over Eu for a range of ligands and proposed a novel ligand with even stronger selectivity.[149]

In addition to investigating the geometry and predicted difference in solvation free energies of metal-ligand complexes, another important role of computation is to understand and help leverage the role of 5*f* valence electrons to improve actinide separations. Recent studies have found that selectivity of dipicolinate with actinides in

3+ oxidation state within the actinide series is correlated with energetic degeneracy between actinide 5*f* and ligand orbitals.[5,150] This is illustrated in Figure 9, which shows how that orbital degeneracy varies across the heavy actinides, explaining intra-actinide selectivity of the ligand. While ligand-metal stability is largely driven by electrostatics, this role of 5*f* electrons presents a unique means to approach some of the more challenging elemental separations with covalent interactions and demonstrates how to leverage information unique to computational methods.

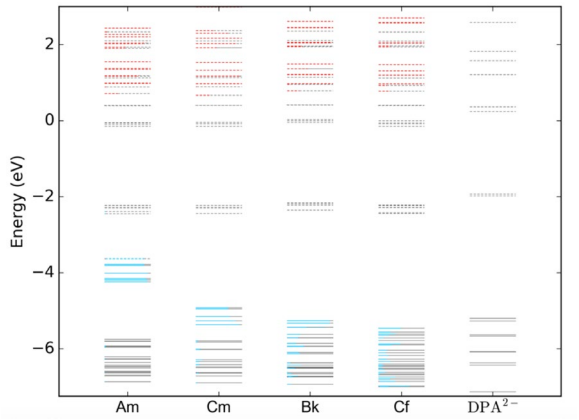

Figure 9: Orbital energetic overlap between 5*f* and 6*d* actinide orbitals and the dipicolinate ligand increases across the heavy actinides from Am to Cf. Red and blue color denote contributions of 5*f* and 6*d* atomic orbitals to the molecular orbitals of the actinide-ligand complex. Reprinted with permission from "On the Origin of Covalent Bonding in Heavy Actinides," Kelley, M. and Su, J. and Urban, M. and Luckey, M. and Batista, E. and Yang, P. and Shafer, J., J. Am. Chem. Soc. 2017, 139, 9901-9908. Copyright 2017 American Chemical Society.

5.6) Outlook

The state-of-the-art in computational chemistry is ever growing, and the same is true for its application to actinide chemistry. Continued advancements in computational capabilities promise to enable even higher accuracy calculations and calculations over larger systems. For the latter case, this will broaden the range of condensed phase chemical phenomenon accessible for studies of *f*-element separations. In particular, the promising accuracy of recent ab initio calculations of simple gas phase actinide clusters may soon extend to larger systems, with larger ligand molecules and realistic solvation. As with many fields of science, the role of predictive modeling in actinide separations will continue to expand.

6) CONCLUSION

Chemical separations of actinides are essential to their effective utilization in domains ranging from medicine to energy production. Here, we reviewed the primary classes of separations processed applied to actinides: adsorption and solid phase extraction, liquid-liquid extraction, and pyroprocessing, with a particular focus on the unique chemical considerations of the actinide elements in each application. Adsorption and solid phase extraction techniques enable multi-stage separations at a benchtop scale. Alternatively, liquid-liquid extraction is ideal for scaling up batch processes and converting them to continuous separation processes. Pyroprocessing eliminates the need for solvents, but only leverages a limited range of chemical behavior to drive separations. Lastly, we discussed computational methods which have been applied broadly to understand the chemistry of the actinides as it relates to those different classes of separations techniques. This article should illustrate the different chemical characteristics leveraged for each separation technique and how they are manipulated to achieve separation between actinides and separation from relevant chemical media.

Acknowledgement

This manuscript has been authored by Savannah River Nuclear Solutions (SRNS), LLC under Contract No. DE-AC09-08SR22470 with the U.S. Department of Energy (DOE) Office of Environmental Management (EM). Disclaimer: The United States Government retains and the publisher, by accepting this article for publication, acknowledges that the United States Government retains a non-exclusive, paid-up,

Related Articles

eibc0001
eibd0653
eibc0251
eibc2525
eibc2528
eibc2529

References

1 G. T. Seaborg, *Chemical & Engineering News Archive*, 1945, **23**, 2190–2193.
2 O. L. Keller, in *Americium and Curium Chemistry and Technology: Papers from a Symposium given at the 1984 International Chemical Congress of Pacific Basin Societies, Honolulu, HI, December 16–27, 1984*, eds. N. M. Edelstein, J. D. Navratil and W. W. Schulz, Springer Netherlands, Dordrecht, 1985, pp. 43–49.
3 N. M. Edelstein, J. Fuger, J. J. Katz and L. R. Morss, in *The Chemistry of the Actinide and Transactinide Elements*, eds. L. R. Morss, N. M. Edelstein and J. Fuger, Springer Netherlands, Dordrecht, 2011, pp. 1753–1835.
4 M. L. Neidig, D. L. Clark and R. L. Martin, *Coord. Chem. Rev.*, 2013, **257**, 394–406.
5 M. P. Kelley, J. Su, M. Urban, M. Luckey, E. R. Batista, P. Yang and J. C. Shafer, *J. Am. Chem. Soc.*, 2017, **139**, 9901–9908.
6 A. G. Baldwin, M. J. Servis, Y. Yang, N. J. Bridges, D. T. Wu and J. C. Shafer, *J. Mol. Liq.*, 2017, **246**, 225–235.
7 M. J. Servis, D. T. Wu and J. C. Braley, *Phys. Chem. Chem. Phys.*, 2017, **19**, 11326–11339.
8 A. G. Baldwin, N. J. Bridges and J. C. Braley, *Ind. Eng. Chem. Res.*, 2016, **55**, 13114–13119.
9 I. Grenthe, J. Drożdżyński, T. Fujino, E. C. Buck, T. E. Albrecht-Schmitt and S. F. Wolf, in *The Chemistry of the Actinide and Transactinide Elements*, eds. L. R. Morss, N. M. Edelstein and J. Fuger, Springer Netherlands, Dordrecht, 2006, pp. 253–698.
10 G. T. Seaborg, *The Plutonium Story*, Lawrence Berkeley Laboratory, 1981.
11 B. Weaver, *Anal. Chem.*, 1954, **26**, 474–475.
12 K. L. Nash and G. R. Choppin, *Sep. Sci. Technol.*, 1997, **32**, 255–274.
13 R. A. Peterson, E. C. Buck, J. Chun, R. C. Daniel, D. L. Herting, E. S. Ilton, G. J. Lumetta and S. B. Clark, *Environ. Sci. Technol.*, 2018, **52**, 381–396.
14 G. K. Allen, *Estimated inventory of chemicals added to underground waste tanks, 1944--1975. [Analysis of sludges and salt cakes]*, Atlantic Richfield Hanford Co., Richland, Wash. (USA), 1976.
15 J. J. Laidler, J. E. Battles, W. E. Miller, J. P. Ackerman and E. L. Carls, *Prog. Nuclear Energy*, 1997, **31**, 131–140.
16 T. Inoue, *Prog. Nuclear Energy*, 2002, **40**, 547–554.
17 T. Inoue, M. Sakata, H. Miyashiro, T. Matsumura, A. Sasahara and N. Yoshiki, *Nucl. Technol.*, 1991, **93**, 206–220.
18 A. Dabrowski, *Adv. Colloid Interface Sci.*, 2001, **93**, 135–224.
19 J. Kammerer, R. Carle and D. R. Kammerer, *J. Agric. Food Chem.*, 2011, **59**, 22–42.
20 R. K. Scopes, in *Protein Purification: Principles and Practice*, ed. R. K. Scopes, Springer New York, New York, NY, 1994, pp. 102–145.
21 E. Rosenberg, G. Pinson, R. Tsosie, H. Tutu and E. Cukrowska, *Johnson Matthey Technology Review*, 2016, **60**, 59–77.
22 C. F. Poole, in *Solid-Phase Extraction*, ed. C. F. Poole, Elsevier, 2020, pp. 1–36.
23 K. A. Kraus, H. O. Phillips, T. A. Carlson and J. S. Johnson, *Ion exchange properties of hydrous oxides*, Oak Ridge National Lab., TN (United States), 1958.
24 I. M. Abrams and J. R. Millar, *React. Funct. Polym.*, 1997, **35**, 7–22.
25 C. B. Amphlett, *Synthetic inorganic ion exchangers and their applications in atomic energy*, Atomic Energy Research Establishment, Harwell, Berks, Eng., 1959.
26 J. R. Millar, D. G. Smith, W. E. Marr and T. R. E. Kressman, *J. Chem. Soc.*, 1963, 218–225.

27 Y. Marcus and A. S. Kertes, *Ion exchange and solvent extraction of metal complexes*, Wiley, 1969.
28 J. L. Ryan and E. J. Wheelwright, *The Recovery, Purification, and Concentration of Plutonium by Anion Exchange in Nitric Acid*, General Electric Co. Hanford Atomic Products Operation, Richland, Wash., 1959.
29 R. A. Glass, *J. Am. Chem. Soc.*, 1955, **77**, 807–809.
30 G. R. Choppin, B. G. Harvey and S. G. Thompson, *J. Inorg. Nucl. Chem.*, 1956, **2**, 66–68.
31 C. W. Abney, R. T. Mayes, T. Saito and S. Dai, *Chem. Rev.*, 2017, **117**, 13935–14013.
32 M. H. Campbell, J. M. Frame, N. D. Dudey, G. R. Kiel, V. Mesec, F. W. Woodfield, S. E. Binney, M. R. Jante, R. C. Anderson and G. T. Clark, *Extraction of uranium from seawater: chemical process and plant design feasibility study*, Bendix Field Engineering Corp., Grand Junction, CO (USA); Exxon Nuclear Co., Inc., Richland, WA (USA); Oregon State Univ., Corvallis (USA). Dept. of Nuclear Engineering; Vitro Engineering Co., New York (USA), 1979.
33 C. Gunathilake, J. Górka, S. Dai and M. Jaroniec, *J. Mater. Chem. A Mater. Energy Sustain.*, 2015, **3**, 11650–11659.
34 J. L. Vivero-Escoto, M. Carboni, C. W. Abney, K. E. deKrafft and W. Lin, *Microporous Mesoporous Mater.*, 2013, **180**, 22–31.
35 M. Carboni, C. W. Abney, K. M. L. Taylor-Pashow, J. L. Vivero-Escoto and W. Lin, *Ind. Eng. Chem. Res.*, 2013, **52**, 15187–15197.
36 T. J. Tranter, in *Advanced Separation Techniques for Nuclear Fuel Reprocessing and Radioactive Waste Treatment*, eds. K. L. Nash and G. J. Lumetta, Woodhead Publishing, 2011, pp. 377–413.
37 E. Philip Horwitz, D. R. McAlister and M. L. Dietz, *Sep. Sci. Technol.*, 2006, **41**, 2163–2182.
38 W. J. de Wet and E. A. C. Crouch, *J. Inorg. Nucl. Chem.*, 1965, **27**, 1735–1744.
39 EPA EMSL, *Method 900.0: Gross Alpha and Gross Beta Radioactivity in Drinking Water. Prescribed procedures for measurement of radioactivity in drinking water*, US Environmental Protection Agency, 1980.
40 W. C. Burnett, D. R. Corbett, M. Schultz, E. P. Horwitz, R. Chiarizia, M. Dietz, A. Thakkar and M. Fern, *J. Radioanal. Nucl. Chem.*, 1997, **226**, 121–127.
41 H. Freiser and G. H. Morrison, *Annu. Rev. Nucl. Sci.*, 1959, **9**, 221–244.
42 H. D. W. Smyth and L. R. Groves, *Atomic energy for military purposes: the official report on the development of the atomic bomb under the auspices of the United States government, 1940-1945*, Princeton University Press, 1945.
43 J. I. Hoffman, *Purification of Uranium Oxide*, Atomic Energy Commission, 1947.
44 B. Weaver and F. A. Kappelmann, *TALSPEAK: A new method of separating americium and curium from the lanthanides by extraction from an aqueous solution of an aminopolyacetic acid complex with a monoacidic organophosphate or phosphonate*, Oak Ridge National Lab., Tenn., 1964.
45 J. Starý, *Talanta*, 1966, **13**, 421–437.
46 B. Weaver and F. A. Kappelmann, *J. Inorg. Nucl. Chem.*, 1968, **30**, 263–272.
47 G. T. Seaborg, *Actinides and Transactinides*, Lawrence Berkeley Lab., 1976.
48 K. C. Sole, M. B. Mooiman and E. Hardwick, *Sep. Purif. Rev.*, 2018, **47**, 159–178.
49 K. C. Sole, P. M. Cole, A. M. Feather and M. H. Kotze, *Solvent Extr. Ion Exch.*, 2011, **29**, 868–899.
50 D. J. Crouse and K. B. Brown, *Recovery of Thorium, Uranium, and Rare Earths from Monazite Sulfate Liquors by the Amine Extraction (Amex) Process*, Oak Ridge National Laboratory, 1959.
51 L. W. Gray, *From separations to reconstitution---A short history of plutonium in the US and Russia*, Lawrence Livermore National Lab., CA (US), 1999.
52 M. S. Gerber, *A Brief History of the PUREX and UO3 Facilities*, Westinghouse Hanford Company, 1993.
53 M. Kamoshida and T. Fukasawa, *J. Nucl. Sci. Technol.*, 1996, **33**, 403–408.

54 B. J. Mincher, L. R. Martin and N. C. Schmitt, *Inorg. Chem.*, 2008, **47**, 6984–6989.
55 B. J. Mincher, L. R. Martin and N. C. Schmitt, *Solvent Extr. Ion Exch.*, 2012, **30**, 445–456.
56 K. McCann, D. M. Brigham, S. Morrison and J. C. Braley, *Inorg. Chem.*, 2016, **55**, 11971–11978.
57 K. McCann, B. J. Mincher, N. C. Schmitt and J. C. Braley, *Ind. Eng. Chem. Res.*, 2017, **56**, 6515–6519.
58 K. McCann, S. I. Sinkov, G. J. Lumetta and J. C. Shafer, *Ind. Eng. Chem. Res.*, 2018, **57**, 1277–1283.
59 K. McCann, S. I. Sinkov, G. J. Lumetta and J. C. Shafer, *New J. Chem.*, 2018, **42**, 5415–5424.
60 J. D. Burns and B. A. Moyer, *Inorg. Chem.*, 2016, **55**, 8913–8919.
61 W. H. Runde and B. J. Mincher, *Chem. Rev.*, 2011, **111**, 5723–5741.
62 F. L. Moore, *Anal. Chem.*, 1963, **35**, 715–719.
63 I. S. Sergey and J. L. Gregg, *Radiochim. Acta*, 2015, **103**, 541–552.
64 C. J. Dares, A. M. Lapides, B. J. Mincher and T. J. Meyer, *Science*, 2015, **350**, 652.
65 K. McCann, J. A. Drader and J. C. Braley, *Sep. Purif. Rev.*, 2018, **47**, 49–65.
66 R. D. Baker, *Preparation of Plutonium Metal by the Bomb Method*, Los Alamos Scientific Laboratory, Los Alamos, NM, 1946.
67 W. Z. Wade and T. Wolf, *The Production of Plutonium Metal by Direct Reduction of the Oxide*, University of California, Livermore, CA, 1968.
68 W. V. Conner, *Reduction of Plutonium Compounds to Plutonium Metal*, The Dow Chemical Company, Golden, CO, 1964.
69 L. J. Mullins and C. L. Foxx, *Direct Reduction of 238PuO2 and 239PuO2 to Metal*, Los Alamos National Laboratory, Los Alamos, NM, 1982.
70 I. L. Jenkins, N. J. Keen and A. G. Wain, *Alternative Routes for the Conversion of Pu Salts to Metal and Their Recovery Problems*, Interscience Publishers, Inc., New York, 1960.
71 J. M. Cleveland, *Plutonium Handbook*, Gordon and Breach Science Publishers, New York, 1967.
72 W. Z. Wade and T. Wolf, *J. Nucl. Sci. Technol.*, 1969, **6**, 402–407.
73 K. W. Fife, D. F. Bowersox, C. C. Davis and E. D. McCormik, *Direct Oxide Reduction (DOR) Solvent Salt Recycle in Pyrochemical Plutonium Recovery Operations*, Los Alamos National Laboratory, Los Alamos, NM, 1987.
74 K. W. Fife, D. F. Bowersox and E. D. McCormick, *Proceedings of The Electrochemical Society*, 1986, 512–521.
75 G. D. Bird, J. McNeese, J. D. Williams, A. J. Vargas and C. W. Thorn, *Automation of MCDOR at NMT-3*, Los Alamos National Laboratory, Los Alamos, NM, 1995.
76 L. J. Mullins, J. A. Leary and W. J. Maraman, *Ind. Eng. Chem. Res.*, 1960, **52**, 227–230.
77 J. B. Knighton and R. K. Steunenberg, *J. Inorg. Nucl. Chem.*, 1965, **27**, 1457–1462.
78 J. D. Navratil, *Journal of the Less Common Metals*, 1984, **100**, 189–194.
79 J. B. Knighton, J. L. Long, R. C. Franchini, R. G. Auge, J. C. Brown and F. G. Meyer, *A Batch Two-Stage Countercurrent Mode for Liquid Plutonium-Molten Salt Extraction of Americium*, Dow Chemical U.S.A., Golden, CO, 1973.
80 J. B. Knighton, R. G. Auge and J. W. Berry, *Molten Salt Extraction of Americium from Molten Plutonium Metal*, Rockwell International, Golden, CO, 1976.
81 M. Kolodney, *Production of Plutonium by Electrolysis*, Los Alamos National Laboratory, 1944.
82 L. J. Mullins and J. A. Leary, *Industrial & Engineering Chemistry Process Design and Development*, 1965, **4**, 394–400.
83 L. J. Mullins, J. A. Leary and A. N. Morgan, *Large Scale Electrorefining of Plutonium from Plutonium-Iron Alloys*, Los Alamos, NM, 1964.
84 L. J. Mullins, J. A. Leary and A. N. Morgan, *Operating Instructions, Procedures, and Equipment for the Los Alamos Plutonium Electrorefining Plant*, Los Alamos Scientific Laboratory, Los Alamos, NM, 1963.
85 L. J. Mullins, J. A. Leary and C. W.

Bjorklund, *Large Scale Preparation of High Purity Plutonium Metal by Electrorefining*, Los Alamos National Laboratory, Los Alamos, NM, 1960.
86 L. J. Mullins, J. A. Leary, A. N. Morgan and W. J. Maraman, *Plutonium Electrorefining*, Los Alamos Scientific Laboratory, Los Alamos, NM, 1962.
87 L. J. Mullins and A. N. Morgan, *A Review of Operating Experience at the Los Alamos Plutonium Electrorefining Facility, 1963-1977*, Los Alamos National Laboratory, Los Alamos, NM, 1981.
88 L. J. Mullins, A. N. Morgan, I. I. I. S. A. Apgar and D. C. Christensen, *Six-Kilogram Scale Electrorefining of Plutonium Metal*, Los Alamos National Laboratory, Los Alamos, NM, 1982.
89 L. B. Pankratz, *Thermodynamic Properties of Halides*, U.S. Department of Interior, Bureau of Mines, 1984.
90 D. C. Christensen, J. D. Williams, J. A. McNeese and K. W. Fife, *Plutonium Metal Preparation and Purification at Los Alamos - 1984*, Los Alamos National Laboratory, Los Alamos, NM, 1985.
91 C. E. Baldwin and J. D. Navratil, in *Plutonium Chemistry*, eds. W. T. Carnall and G. R. Choppin, American Chemical Society, Washington, D. C., 1983, pp. 369–380.
92 D. C. Christensen and L. J. Mullins, in *Plutonium Chemistry*, eds. W. T. Carnall and G. R. Choppin, American Chemical Society, Washington, D.C., 1983, pp. 409–431.
93 J. L. Long and R. D. Schweikhardt, *Plutonium Electrorefining at Rocky Flats*, Dow Chemical Company, Golden, CO, 1967.
94 S. Owens, K. Axler, G. Bird, M. Reimus, E. Garcia and G. DePoorter, *ECS Proceedings Volumes*, 1992, **16**, 204–214.
95 A. H. Jones, T. J. Paget and R. F. Watson, *ECS Proceedings Volumes*, 2004, **2004-24**, 749–760.
96 D. Lambertin, S. Ched'homme, G. Bourgès, S. Sanchez and G. Picard, *J. Nucl. Mater.*, 2005, **341**, 124–130.
97 D. Lambertin, S. Ched'homme, G. Bourgès, L. Pescayre, S. Sanchez and G. Picard, *ECS Proceedings Volumes*, 2004, **24**, 700–712.
98 J. L. Willit, W. E. Miller and J. E. Battles, *J. Nucl. Mater.*, 1992, **195**, 229–249.
99 E.-Y. Choi and S. M. Jeong, *Progress in Natural Science: Materials International*, 2015, **25**, 572–582.
100 M. F. Simpson, *Developments of Spent Nuclear Fuel Pyroprocessing Technology at Idaho National Laboratory*, United States, 2012.
101 F. H. Driggs and W. C. Lilliendahl, *Ind. Eng. Chem. Res.*, 1930, **22**, 516–519.
102 C. Marzano and R. A. Noland, *The Electrolytic Refining of Uranium*, Argonne National Laboratory, 1953.
103 D. Inman, G. J. Hills, L. Young and J. O. Bockris, *Transactions of the Faraday Society*, 1959, **55**, 1904–1914.
104 G. Boisdie, G. Chauvin, H. Coriou and J. Hure, *Electrochim. Acta*, 1961, **5**, 54–71.
105 G. Chauvin, H. Coriou and A. Simenauer, *Electrochim. Acta*, 1963, **8**, 323–332.
106 D. L. Hill, J. Perano and R. A. Osteryoung, *J. Electrochem. Soc.*, 1960, **107**, 698.
107 L. Martinot, T. Gérard and G. Duyckaerts, *Inorganic and Nuclear Chemistry Letters*, 1973, **9**, 657–665.
108 G. Chauvin, H. Coriou, P. Jabot and A. Laroche, *J. Nucl. Mater.*, 1964, **11**, 183–192.
109 M. Kolodney, *J. Electrochem. Soc.*, 1982, **129**, 2438–2442.
110 L. W. Niedrach and B. E. Dearing, *J. Electrochem. Soc.*, 1958, **105**, 353.
111 R. D. Piper and R. F. Leifield, *Industrial & Engineering Chemistry Process Design and Development*, 1962, **1**, 208–212.
112 K. Gourishankar, L. Redey and M. Williamson, *Light Metals: Proceedings of Sessions, TMS Annual Meeting (Warrendale, Pennsylvania)*.
113 M. A. Williamson and J. Willit, *Nuclear Engineering and Technology*, , DOI:10.5516/NET.2011.43.4.329.
114 S. D. Herrmann, S. X. Li, M. F. Simpson and S. Phongikaroon, *Sep. Sci. Technol.*, 2006, **41**, 1965–1983.
115 S. D. Herrmann, S. X. Li and B. R. Westphal, *Sep. Sci. Technol.*, 2012, **47**, 2044–2059.

116 S. X. Li, S. D. Herrmann and M. F. Simpson, *Nucl. Technol.*, 2010, **171**, 292–299.
117 W. Küchle, M. Dolg, H. Stoll and H. Preuss, *J. Chem. Phys.*, 1994, **100**, 7535–7542.
118 A. Kovács, R. J. M. Konings, J. K. Gibson, I. Infante and L. Gagliardi, *Chem. Rev.*, 2015, **115**, 1725–1759.
119 V. Vallet, P. Macak, U. Wahlgren and I. Grenthe, *Theor. Chem. Acc.*, 2006, **115**, 145–160.
120 M. Duvail, F. Martelli, P. Vitorge and R. Spezia, *J. Chem. Phys.*, 2011, **135**, 044503.
121 P. D'Angelo, F. Martelli, R. Spezia, A. Filipponi and M. A. Denecke, *Inorg. Chem.*, 2013, **52**, 10318–10324.
122 R. Spezia, V. Migliorati and P. D'Angelo, *J. Chem. Phys.*, 2017, **147**, 161707.
123 P. Li and K. M. Merz Jr, *J. Chem. Theory Comput.*, 2014, **10**, 289–297.
124 P. Li, L. F. Song and K. M. Merz Jr, *J. Chem. Theory Comput.*, 2015, **11**, 1645–1657.
125 P. Li, L. F. Song and K. M. Merz Jr, *J. Phys. Chem. B*, 2015, **119**, 883–895.
126 A. Marjolin, C. Gourlaouen, C. Clavaguéra, P. Y. Ren, J.-P. Piquemal and J.-P. Dognon, *J. Mol. Model.*, 2014, **20**, 2471.
127 M. Montagna, R. Spezia and E. Bodo, *Inorg. Chem.*, 2017, **56**, 11929–11937.
128 J. W. Ponder, C. Wu, P. Ren, V. S. Pande, J. D. Chodera, M. J. Schnieders, I. Haque, D. L. Mobley, D. S. Lambrecht, R. A. DiStasio Jr and Others, *J. Phys. Chem. B*, 2010, **114**, 2549–2564.
129 J. Song, S. Shi, X. Li and L. Yan, *J. Mol. Liq.*, 2017, **234**, 279–286.
130 C. Bessada, D. Zanghi, M. Salanne, A. Gil-Martin, M. Gibilaro, P. Chamelot, L. Massot, A. Nezu and H. Matsuura, *J. Mol. Liq.*, 2020, 112927.
131 B. Li, S. Dai and D.-E. Jiang, *J. Mol. Liq.*, 2020, **299**, 112184.
132 A. Klamt, *WIREs Comput Mol Sci*, 2011, **1**, 699–709.
133 C.-M. Hsieh, S. I. Sandler and S.-T. Lin, *Fluid Phase Equilib.*, 2010, **297**, 90–97.
134 I. Infante and L. Visscher, *J. Comput. Chem.*, 2004, **25**, 386–392.
135 S. O. Odoh, S. M. Walker, M. Meier, J. Stetefeld and G. Schreckenbach, *Inorg. Chem.*, 2011, **50**, 3141–3152.
136 A. P. Ladshaw, A. S. Ivanov, S. Das, V. S. Bryantsev, C. Tsouris and S. Yiacoumi, *ACS Appl. Mater. Interfaces*, 2018, **10**, 12580–12593.
137 P. Guilbaud, L. Berthon, W. Louisfrema, O. Diat and N. Zorz, *Chemistry*, 2017, **23**, 16660–16670.
138 M. J. Servis, D. T. Wu, J. C. Shafer and A. E. Clark, *Chem. Commun.* , 2018, **54**, 10064–10067.
139 P. K. Mohapatra, *Dalton Trans. J. Inorg. Chem.*, 2017, **46**, 1730–1747.
140 I. A. Shkrob, T. W. Marin and M. P. Jensen, *Ind. Eng. Chem. Res.*, 2014, **53**, 3641–3653.
141 K. A. Maerzke, G. S. Goff, W. H. Runde, W. F. Schneider and E. J. Maginn, *J. Phys. Chem. B*, 2013, **117**, 10852–10868.
142 I. V. Leontyev and A. A. Stuchebrukhov, *J. Chem. Phys.*, 2009, **130**, 02B609.
143 A. Chaumont and G. Wipff, *Phys. Chem. Chem. Phys.*, 2006, **8**, 494–502.
144 M. Vasiliu, T. Jian, J. K. Gibson, K. A. Peterson and D. A. Dixon, *Inorg. Chem.*, 2020, **59**, 4554–4566.
145 R. Feng, E. D. Glendening and K. A. Peterson, *Inorg. Chem.*, 2020, **59**, 4753–4763.
146 M. Vasiliu, J. K. Gibson, K. A. Peterson and D. A. Dixon, *Chem.--Eur. J.*, 2019, **25**, 4245–4254.
147 A. Kovács, P. Pogány and R. J. M. Konings, *Inorg. Chem.*, 2012, **51**, 4841–4849.
148 C.-Z. Wang, J.-H. Lan, Q.-Y. Wu, Y.-L. Zhao, X.-K. Wang, Z.-F. Chai and W.-Q. Shi, *Dalton Trans. J. Inorg. Chem.*, 2014, **43**, 8713–8720.
149 V. S. Bryantsev and B. P. Hay, *Dalton Trans. J. Inorg. Chem.*, 2015, **44**, 7935–7942.
150 M. P. Kelley, G. J.-P. Deblonde, J. Su, C. H. Booth, R. J. Abergel, E. R. Batista and P. Yang, *Inorg. Chem.*, 2018, **57**, 5352–5363.